FEDERAL UNIVERSITY OF CEARÁ

CENTER OF TECHNOLOGY

TELEINFORMATICS ENGINEERING DEPARTMENT

POSTGRADUATE COURSE IN TELEINFORMATICS ENGINEERING

INTERFERENCE MITIGATION WITH BASE STATION COOPERATION IN MULTICELL MULTIUSER WIRELESS SYSTEMS

Velser Darllan Benício Correia

Fortaleza - Ceará

November 2009

FEDERAL UNIVERSITY OF CEARÁ

CENTER OF TECHNOLOGY

TELEINFORMATICS ENGINEERING DEPARTMENT

POSTGRADUATE COURSE IN TELEINFORMATICS ENGINEERING

INTERFERENCE MITIGATION WITH BASE STATION COOPERATION IN MULTICELL MULTIUSER WIRELESS SYSTEMS

Author:

Velser Darllan Benício Correia

Supervisor:

Prof. Dr. Yuri Carvalho Barbosa da Silva

Co-supervisor:

Prof. Dr. Francisco Rodrigo Porto Cavalcanti

Thesis submitted to the Coordination of the Graduate Program in Teleinformatics Engineering of the Federal University of Ceará as part of the requirements for obtaining the ***Master's degree in Teleinformatics Engineering***

Fortaleza - Ceará

November 2009

Abstract

This Master's dissertation tackles the problem of interference mitigation in multi-cell multi-user wireless communication scenarios where a ditributed MIMO structure can be made feasible by assuming that a perfect BS cooperation is allowed. Performance evaluation of different interference mitigation approaches is assessed.

By considering a set of cooperative BSs as a joint MIMO transmitter, streams intended to a set of co-channel MSs can be spread across all transmit antennas and hence, precoding techniques can be fully applied to suppress co-channel interference. The performance of different linear and non-linear precoding techniques is evaluated, taking also into account scenarios with imperfect channel estimation.

Additionally to precoding techniques, inter-cell scheduling is discussed as well as the application of both approaches together, but yet decoupled from each other.

As a step further, this work extends previous studies on the theme of BS cooperation by taking into account the impact of size-limited cooperation groups (each cooperation group is, in fact, a cluster in the overall grid) in a system-wide cellular deployment and by proposing an efficient joint scheduling and precoding algorithm. The proposed algorithm takes into account the out-of-cluster interference and is shown to outperform other strategies, while still presenting a low computational complexity.

Contents

List of Figures

List of Tables

Chapter 1

Introduction

The present dissertation addresses the problem of interference management in a cooperative multi-cell multi-user scenario with Multiple Input Multiple Output (MIMO) structures.

Receive processing has been considered to cope with the distortions caused by the channel, where the receive filter is adapted to the channel properties and the *a priori* known transmit filter. The most attractive point on receive processing is the easy Channel State Information (CSI) acquisition by the use of known training symbols transmitted together with the unknown data. Despite the benefits provided by such an approach a reasonable receiver complexity has shown to be a constant issue. On the other hand, transmit processing can drastically reduce receiver complexity by moving the burden to the transmitter side. This technique can, in many cases, reduce the receive processing to a scalar filter, in many cases. Many receive processing techniques had their optimization problems adapted to their equivalent ones in the transmitter side.

This dissertation assumes that BSs are able to cooperate in the transmitter side in order to provide a joint transmit strategy to deal with the interference.

The theme of BS cooperation (or coordination) in cellular networks has been the subject of several recent studies [1–5], which anticipate promising gains in terms of spectral efficiency for the next generation of wireless systems. In this context, by cooperation/coordination it is meant that there is a Cluster Processing Unit (CPU) capable of controlling a certain number of BSs, which allows the implementation of advanced techniques for managing the interference in the network.

Assuming that the CPU has access to the channel measurements of all Mobile Stations (MSs) associated to a group of cooperating BSs, it is possible to apply inter-cell scheduling and resource allocation techiques that aim at maximizing the spectral efficiency given the estimated interference within this group, such as proposed in [1–3].

Another technique that can benefit from this sort of cooperation is the so-called Virtual Antenna

Array (VAA), also known as network MIMO or distributed precoding, in which a precoded version of the transmit symbols are sent from the cooperating BSs such that the intra-group interference can be mitigated. Recent works have analysed the performance of different precoding techniques in a cooperative scenario, such as [4]. In [5] system-wide cooperation is assumed and compared to the case without cooperation, showing that huge gains can be achieved.

The problem which is the main point of this work is finding an approach to improve the average cell throuput in this scenario compared to conventional scheduling and precoding solutions.

1.1 Motivation

The aforementioned studies, however, present some problems and disadvantages, which might prevent them from exploiting the full potential of BS cooperation.

One problem is that the inter-cell scheduling and distributed precoding techniques are often treated as separate strategies. The scheduler selects MSs according to certain criteria, which do not take into account the spatial compatibility, i.e., whether it is possible to efficiently cancel the inter-MS interference by means of precoding.

Another relevant issue concerns the impact of the out-of-group interference on the performance of the cooperative strategies. Since it is assumed that the CPU controlling the cooperation group only has information about the links within the group, the interference coming from outside has not been taken into account by existing solutions, even though it might be strong enough to impact performance. These existing solutions have assumed that there is no outside interference whatsoever, or it is assumed that the whole system cooperates, which are two extreme cases.

1.2 Contributions

In this dissertation two algorithms are proposed in order to take advantage of scheduling and precoding techniques in a combined approach. They offer reasonable complexity and higher gains compared to conventional algorithms.

It is assumed that all BSs inside a cluster keep a perfect cooperation. Such a cooperation aims at providing all channel information regarding all MSs within a cooperation group, hereafter a cluster. The main objective is to maximise the sum capacity inside each cluster.

The first algorithm, called Precoding-Aware Non-Orthogonal Inter-Cell Scheduler (PANOIS), applies a precoder to a set of scheduled MSs. This MS scheduling is done by using heuristic search methods so as to avoid impracticable complexity due to exaustive searchs. The second,

Interference-Adaptive Precoding-Aware Non-Orthogonal Inter-Cell Scheduler (IAPANOIS), is an extension of the first and additionally it is aware of the out-of-cluster interference, which was shown to impact significantly on the cluster sum capacity.

1.3 Notation

Table 1.1: Most Frequent Operators

Operator	Description
$\mathrm{E}[\bullet]$	Expectation
$\|\bullet\|_2$	Euclidian norm of a vector
$\|\bullet\|_F$	Frobenius norm of a vector
$\mathrm{tr}(\bullet)$	Trace of a matrix
$[\bullet]^{-1}$	Matrix inversion
$\mathrm{diag}(\bullet)$	Vector of the diagonal elements of a matrix arguments
$\bullet^H$	Conjugate transposition

1.4 Organization of this work

This dissertation is divided in five chapters. The content of each chapter is stated above.

- **Chapter 2: Base Station Cooperation** This chapter describes the model which all simulations are based on. Some issues concerning the scenario, like number of antennas, number of MSs per cell, number of cells, size of cooperation groups and cluster topologies are covered;

- **Chapter 3: Interference Management** In this chapter an overview of conventional interference mitigation techniques considered in this work is presented. At the end of this chapter some results ilustrates the gains achieved by these techniques.

- **Chapter 4: Combined Inter-Cell Scheduling and Precoding** In this chapter our two proposed algorithms, PANOIS and IAPANOIS are discussed in details. At the end simulation results illustrate the gains obtained with them.

- **Chapter 5: Conclusions** In this chapter, the final conclusions and perpectives are drawn.

Chapter 2

Base Station Cooperation

Considering a multicell multi-user scenario, a cooperative exchange of information among BSs could be explored, and that is where *base station cooperation* takes place. In the current infrastructure of cellular communication systems and indoor wireless internet access, BSs and Access Points (APs) are connected by a high-speed wired backbone that allows reliable exchange of information, making this approach of using cooperating BSs a feasible one.

The scenario used in this work consists of several clusters, where BS cooperation exists only inside each one. There is no cooperation among clusters, but the interference among them is taken into account, differently from previous studies such as [4]. Each BS and MS may be equipped with more than one antenna element depending on the analysis being carried on. It is important to mention that wrap-around has been considered in the grid generation of this work, with the purpose of having a more realistic scenario without border effects.

It is indispensable to emphasize here that a *cluster* in this work means a group where BS cooperation is allowed within. According to this statement a cluster may be formed by several cooperating cells placed far apart from each other in the grid plan, not requiring to be necessarily adjacent to each other as in the classical view of a cluster. Another relevant point is the way a group of BSs is considered to be a cluster by the system. Some examples are pointed in the following. One possible way is to set up a control protocol to manage downlink transmission among cooperative BSs as ilustrated in Fig. 2.1(a). This case is the distributed cooperative scenario where there is no central processing element within the cluster. Another possibility could be the one depicted in Fig. 2.1(b) where adjacent BSs can cooperate through a CPU which is responsible to decide upon the transmission of all cooperative BSs in the downlink. One step much further could be the case where full cooperation is allowed in the entire grid of cells assuming it to be an unique cluster. This last situation is ilustrated in Fig. 2.1(c) and is less realistic or at least

much challengeful than the case in Fig. 2.1(b) once the amount of signalling among cooperative BSs is hardly increased, demanding a more computational-powerful hardware in the CPU to deal with such a task compared to the small-scale case in Fig. 2.1(b) with a reasonable number of cooperative BSs. The distributed cooperation scenario has the advantage to be cheaper than these two last concerning extra hardware deployment to centralize the processing.

The simulation results presented in this work assumed the cluster topology depicted in Fig. 2.1(b).

2.1 System Model

Let us consider the signal model within each cooperation group. Let K represent the total number of MSs within each group, N_{b} the number of BSs within each group, N_{r} the number of receive antennas of each MS, N_{t} the number of transmit antennas of each BS, N_{R} the total number of receive antennas and N_{T} the total number of transmit antennas within the group. It is considered that all transmission is under flat fading and that the channel is slow enough so as the time references can be negleted in our equations in this work. The assumption of perfect BS cooperation allows for conceiving a joint channel matrix $\mathbf{H} \in \mathbb{C}^{N_{\mathrm{R}} \times N_{\mathrm{T}}}$ as in [4] which can be written as

$$\mathbf{H} = \begin{bmatrix} \mathbf{H}_{1,1} & \mathbf{H}_{1,2} & \cdots & \mathbf{H}_{1,N_{\mathrm{b}}} \\ \mathbf{H}_{2,1} & \mathbf{H}_{2,2} & \cdots & \mathbf{H}_{2,N_{\mathrm{b}}} \\ \vdots & \vdots & \ddots & \vdots \\ \mathbf{H}_{N_{\mathrm{u}},1} & \mathbf{H}_{N_{\mathrm{u}},2} & \cdots & \mathbf{H}_{N_{\mathrm{u}},N_{\mathrm{b}}} \end{bmatrix}, \tag{2.1}$$

where $\mathbf{H}_{i,j} \in \mathbb{C}^{N_{\mathrm{R},i} \times N_{\mathrm{T},j}}$ contains the MIMO channel coefficients between BS j and MS i.

Mathematically, as illustrated in Fig. 2.2, all transmission is modeled as

$$\mathbf{y} = \mathbf{GHTs} + \mathbf{Gn}\,, \tag{2.2}$$

where $\mathbf{s} \in \mathbb{C}^{N_{\mathrm{R}}}$ is the *joint transmit vector*, $\mathbf{T} \in \mathbb{C}^{N_{\mathrm{T}} \times N_{\mathrm{R}}}$ is the *joint precoding matrix*, $\mathbf{H} \in \mathbb{C}^{N_{\mathrm{R}} \times N_{\mathrm{T}}}$ is the *joint channel matrix*, $\mathbf{G} \in \mathbb{C}^{N_{\mathrm{R}} \times N_{\mathrm{R}}}$ is a block diagonal matrix representing the processing – when needed – done at each MS, and $\mathbf{n} \in \mathbb{C}^{N_{\mathrm{R}}}$ is the Additive White Gaussian Noise (AWGN) perceived at each receive antenna element. When scheduling techniques are applied before precoding, the joint transmit vector $\mathbf{s}$ is now intended to the scheduled MSs only, which was neither regarded in [4] nor [5]. For (2.2), it is assumed that the total number of data streams is

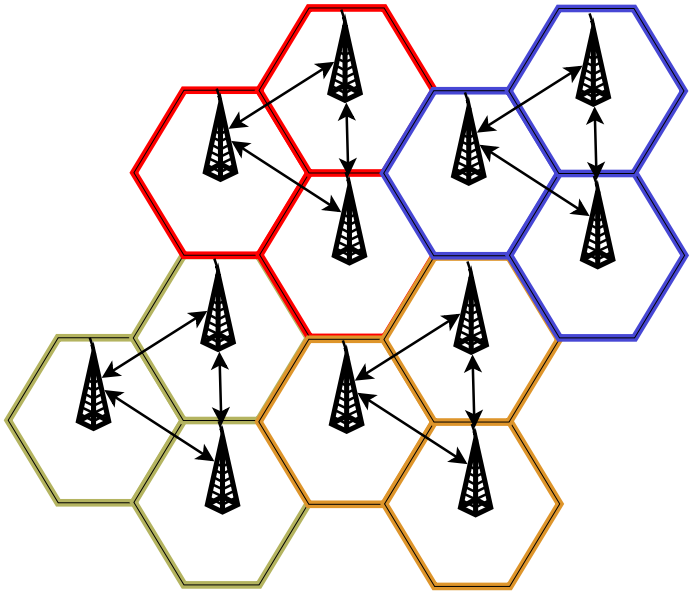

(a) Distributed cooperation scenario

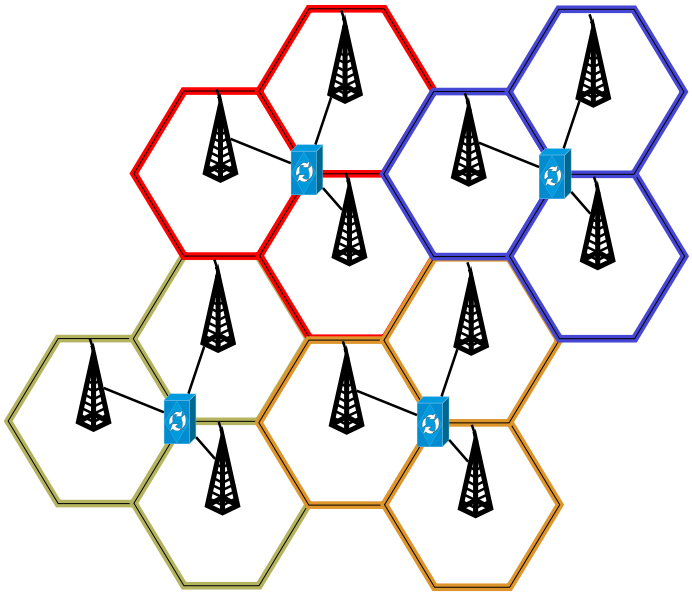

(b) Adjacent-cells cooperation scenario

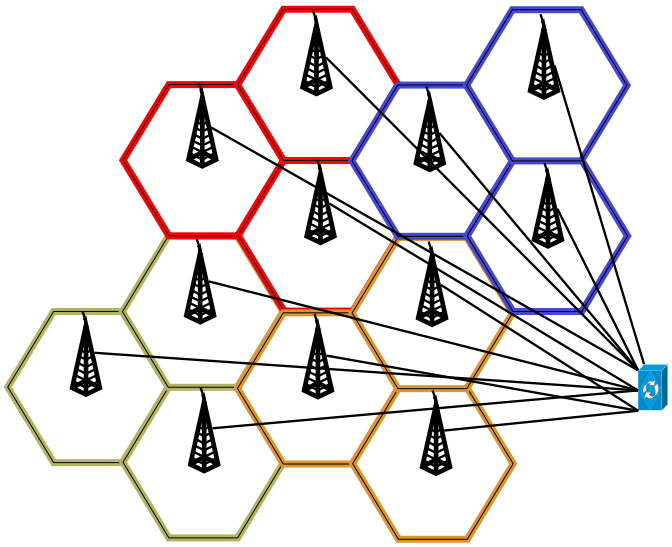

(c) Full cooperation scenario

Figure 2.1: Examples of different possible cluster topologies

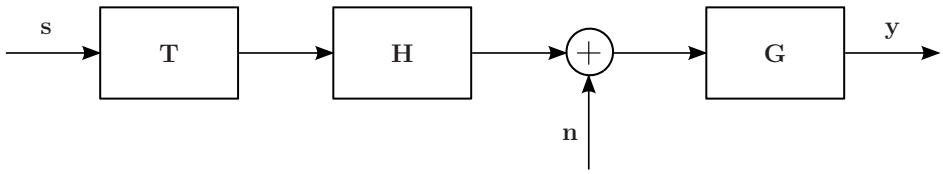

Figure 2.2: MIMO system as a filter chain.

equal to N_{R} and that $N_{\mathrm{T}} \geqslant N_{\mathrm{R}}$.

The joint precoding matrix $\mathbf{T}$, which is designed based on the channel matrix $\mathbf{H}$, can be seen as a product of the following two matrices:

$$\mathbf{T} = \mathbf{P}\mathbf{\Omega}\,, \tag{2.3}$$

where $\mathbf{P} \in \mathbb{C}^{N_{\mathrm{T}} \times N_{\mathrm{R}}}$ is the matrix which actually performs the precoding technique and $\mathbf{\Omega} \in \mathbb{R}^{N_{\mathrm{R}} \times N_{\mathrm{R}}}$ is a matrix that may perform a more accurate power allocation or just a power normalization. The power normalization used in this work is given by

$$\mathbf{\Omega} = \left(\min_{j=1,2,\ldots,N_{\mathrm{b}}} \sqrt{\frac{P_j}{||\mathbf{P}^{[j]}||_{\mathrm{F}}^2}} \right) \mathbf{I}\,. \tag{2.4}$$

where P_j is the power constraint of BS j, $\mathbf{P}^{[j]} \in \mathbb{C}^{N_{\mathrm{t}} \times N_{\mathrm{R}}}$ is the matrix obtained considering the rows of $\mathbf{P}$ corresponding to BS j, $||\cdot||_{\mathrm{F}}$ is the Frobenius norm of a matrix, and $\mathbf{I}$ is an identity matrix of proper dimensions. This power normalization was also applied in [6], which normalizes based on the BS requiring the highest amount of power, i.e., the most power-demanding BS transmits at its maximum available power while the other ones are scaled down accordingly.

Note that this group signal model can be extended to the whole cell grid. The dimensions of the vectors and matrices in (2.2) are expanded to include the whole system. The $\mathbf{y}$, $\mathbf{s}$, and $\mathbf{n}$ vectors of each group are simply stacked upon each other, $\mathbf{G}$ is a square matrix considering all receive antennas in the system, the channel matrix $\mathbf{H}$ now takes into account all links within the system, including those which cross group boundaries, and $\mathbf{T}$ also has a parcel accounting for out-of-group interactions. Since the precoding design is done assuming cooperation only within each group, the system-wide matrix $\mathbf{T}_{\mathrm{sys}}$ is actually block diagonal, i.e., the out-of-group interference is not cancelled. For example, assuming two cooperation groups, the $\mathbf{H}_{\mathrm{sys}}$ and $\mathbf{T}_{\mathrm{sys}}$ matrices can be written as

$$\mathbf{H}_{\mathrm{sys}} = \begin{bmatrix} \mathbf{H}_{1,1} & \mathbf{H}_{1,2} \\ \mathbf{H}_{2,1} & \mathbf{H}_{2,2} \end{bmatrix}, \quad \mathbf{T}_{\mathrm{sys}} = \begin{bmatrix} \mathbf{T}_{1,1} & \mathbf{0} \\ \mathbf{0} & \mathbf{T}_{2,2} \end{bmatrix}. \tag{2.5}$$

The cross channel submatrix $\mathbf{H}_{i,j}$ represents the links between users of group i and the BSs of

group j. The precoder $\mathbf{T}_{i,i}$ is designed based only on $\mathbf{H}_{i,i}$, therefore $\mathbf{T}_{i,j} = \mathbf{0}$ for $i \neq j$. When multiplying $\mathbf{H}_{\text{sys}}$ and $\mathbf{T}_{\text{sys}}$ for calculating the Signal to Interference plus Noise Ratio (SINR), the interference among groups is found in the $\mathbf{H}_{1,2}\mathbf{T}_{2,2}$ and $\mathbf{H}_{2,1}\mathbf{T}_{1,1}$ submatrices.

2.2 Spectral Efficiency Calculation

After applying precoding to the channel a resulting equivalent channel $\mathbf{H}_{\text{eq}} = \mathbf{HT}$ can be considered. Then, the SINR at each receive antenna i can be calculated by

$$\text{SINR}_i = \frac{|\mathbf{H}_{\text{eq}_{i,i}}|^2}{\sum_{j \neq i} |\mathbf{H}_{\text{eq}_{i,j}}|^2 + P_{noise}}, \tag{2.6}$$

2.3 Some Advantages

Besides the capability for Co-Channel Information (CCI) mitigation, some other advantages of using BS cooperation are:

- **Channel rank and conditioning**

  Assuming BS cooperation in a multicell MIMO system, the overall transmit array is distributed among cooperative BSs. By doing this all subchannel matrices corresponding to the transmission from each BS to a certain MS j $\{\mathbf{H}_{b,j}\}$ $(b = 1, \ldots, N_b)$ are independent to each other. So, the total number of independent links is given by $\sum_{b=1}^{N_b} rank\left(\mathbf{H}_{b,j}\right)$ which is assured to be at least equal to N_b. And therefore, if $N_b \geqslant N_r$ the overall channel seen by the MS j, $\mathbf{H}_{Ej} = [\mathbf{H}_{1,j}, \mathbf{H}_{2,j}, \mathbf{H}_{3,j}, \ldots, \mathbf{H}_{N_b,j}] \in \mathbb{C}^{N_{\text{r}} \times N_{\text{t}} N_{\text{b}}}$, will always be full-rank. Moreover, even if local fading occurs at each BS, the channel conditioning will not be greatly degraded as the fading among different transmit antennas at different BSs is still uncorrelated.

- **Macrodiversity protection against shadowing**

  Shadowing is a position-dependent factor and thus transmit antennas placed at the same BS are generally subject to the same attenuation. For noncooperative MIMO BSs, strong shadowing conditions may degrade the capacity significantly. On the other hand, BS cooperation can offer macrodiversity protection for shadowing impairments as BSs are independent to each other and consequently there is a much lower probability that all antennas be under deep fading compared to the case where the entire antenna array is co-located at the same BS (noncooperative scenario).

Chapter 3

Performance of Cooperative Precoding

This chapter aims at discussing the precoding algorithms considered in this work in order to provide insights into the proposed approach presented in chapter 4. It is organized in four sections, being the first about precoding techniques and the latter about precoding ones.

3.1 Precoding Techniques

Precoding algorithms can be divided into linear and non-linear. The linear precoders considered here are: Matched Filter (MF), Zero-Forcing (ZF), Minimum Mean Square Error (MMSE) and Block Diagonalization (BD), whereas the non-linear precoders are Zero-Forcing based Tomlinson-Harashima Precoder (ZF-THP) and QR decomposition based Successive Interference Cancellation (QRSIC). Each of them is decribed in the following. For convenience, in this chapter consider that the receive vector (all received symbols stacked up each other in a vector) is given as follows

$$\mathbf{y} = \mathbf{GHPs} + \mathbf{Gn}\,, \tag{3.1}$$

where each variable but the matrix $\mathbf{P}$ has the same meaning as in eq. (2.2). The matrix $\mathbf{P}$ used in the analytical expressions of the precoders reviewed in this chapter is a transmit filter that takes into account a pooled power constraint which is not realistic for the purpose of this work, where the individual power constraint of each BS is supposed to be regarded. As a suboptimal solution to this problem the scaling factor concerning the pooled power constraint presented in the analytical expressions of the precoders used in this work is removed, turning the resulting precoder $\mathbf{P}$ to be that one in eq. (2.2); after that a simple power normalization regarding the per-BS power constraints is applied by the $\mathbf{\Omega}$ matrix as shown in eq. (2.3). This modeling approach is based on that one in [4].

All precoders shown in this section assume that the receive processing $\mathbf{G}$ in eq. (3.1) is an scalar filter with the exception of BD precoder which assumes that $\mathbf{G}$ is a receive ZF filter. Hence, $\mathbf{G}$ will be hereafter omited in this text. Additionally, it is assumed that the *joint transmitter* has complete knowledge of the channel $\mathbf{H}$ and the input covariance matrix $\mathbf{R}_{\mathrm{s}}$, as well as the receive processing $\mathbf{G}$.

It is not intended to provide the mathematical proofs involved in each precoder derivation but only to cover the main expressions concerning each of them. The insterested reader can find further information about linear precoding in [7] and [8] for instance. Theory and results regarding non-linear precoding can be found in [9–13] for example. Additionally, linear and non-linear precoding are both well discussed in [14] and [15]. All expressions here assume a slow-varying channel which allows us to omit time references in all of them.

3.1.1 Matched Filter (MF)

The MF consists of a filter that maximizes SNR at the filter output. As it does not regard interference it is optimum for noise-limited scenario. The optimization problem for the MF is stated below.

$$\mathbf{P}_{\mathrm{MF}} = \underset{\mathbf{P}}{\operatorname{argmax}} \frac{\left|\mathrm{E}\left[\mathbf{s}^H\mathbf{y}\right]\right|^2}{\mathrm{E}\left[\|\mathbf{n}\|_2^2\right]} \quad \text{s.t.} \quad \mathrm{E}\left[\|\mathbf{P}\mathbf{s}\|_2^2\right] = \mathrm{E}_{\mathrm{T}} \ . \tag{3.2}$$

where E_{T} is the available transmit power.

The solution to this problem is given below

$$\mathbf{P}_{\mathrm{MF}} = \beta_{\mathrm{MF}}\mathbf{H}^H \in \mathbb{C}^{N_{\mathrm{T}} \times N_{\mathrm{R}}} , \tag{3.3}$$

where β_{MF} is a real scaling factor given in eq. (3.4), regarding a pooled power constraint.

$$\beta_{\mathrm{MF}} = \sqrt{\frac{\mathrm{E}_{\mathrm{T}}}{\mathrm{tr}\left(\mathbf{H}^H\mathbf{R}_{\mathrm{s}}\mathbf{H}\right)}} . \tag{3.4}$$

3.1.2 Zero-Forcing (ZF)

With the knowledge of the channel $\mathbf{H}$ it is possible to go further than MF by removing completely the interference caused by the transmitter. Such a transmit filter can be designed by forcing the chain formed by the precoder $\mathbf{P}$, the channel $\mathbf{H}$ and the receive processing $\mathbf{G}$ to be the identity mapping:

$$\mathbf{H}\mathbf{P} = \mathbf{I}_{\mathrm{R}} . \tag{3.5}$$

By doing this, all perturbation caused by the transmitter is removed, i.e. the interference, once the transmitter has no influence on the noise at receiver. So the transmit power must be minimised instead of the noise power at receiver, as below

$$\mathbf{P}_{\text{ZF}} = \underset{\mathbf{P}}{\operatorname{argmin}} \, \mathrm{E}\left[\|\mathbf{Ps}\|_2^2\right] \quad \text{s.t.} \quad \mathbf{HP} = \mathbf{I}_{\text{R}} \,, \tag{3.6}$$

By making use of Lagrange multipliers the following expression can be reached

$$\mathbf{P}_{\text{ZF}} = \mathbf{H}^H \left(\mathbf{HH}^H\right)^{-1} \in \mathbb{C}^{N_{\text{T}} \times N_{\text{R}}} \,, \tag{3.7}$$

which represents the unconstrained transmit power form of the ZF filter. By heuristically inserting a scaling factor β_{ZF} given in eq. (3.8) to take into account the power constraint at the transmitter the final expression for the ZF precoder becomes the one in eq. (3.9).

$$\beta_{\text{ZF}} = \sqrt{\frac{\mathrm{E}_{\text{T}}}{\operatorname{tr}\left((\mathbf{HH}^H)^{-1}\mathbf{R}_{\text{s}}\right)}} \,, \tag{3.8}$$

$$\mathbf{P}_{\text{ZF}} = \beta_{\text{ZF}} \mathbf{H}^H \left(\mathbf{HH}^H\right)^{-1} \in \mathbb{C}^{N_{\text{T}} \times N_{\text{R}}} \,. \tag{3.9}$$

3.1.3 Minimum Mean Square Error (MMSE)

The MMSE precoder is a transmit filter that meets the trade-off between minimizing the transmit power (as done by ZF) and maximizing the SNR at the receiver (as done by MF). This is achieved by allowing some portion of the interference to remain in order to increase the received power of the desired signal. The derivation of the MMSE precoder is closely related to Wiener optimization and thus results from the Mean Square Error (MSE) minimization below

$$\mathbf{P}_{\text{MMSE}} = \underset{\mathbf{P}}{\operatorname{argmin}} \, \mathrm{E}\left[\|\mathbf{s} - \mathbf{y}\|_2^2\right] \quad \text{s.t.} \quad \mathrm{E}\left[\|\mathbf{Ps}\|_2^2\right] \leq \mathrm{E}_{\text{T}} \,. \tag{3.10}$$

With the Lagrange multipliers method the final expression is found

$$\mathbf{P}_{\text{MMSE}} = \beta_{\text{MMSE}} \left(\mathbf{H}^H \mathbf{G}^H \mathbf{GH} + \lambda \mathbf{I}_{N_{\text{R}}}\right)^{-1} \mathbf{H}^H \mathbf{G}^H \in \mathbb{C}^{N_{\text{T}} \times N_{\text{R}}} \,, \tag{3.11}$$

where the scaling factor β_{MMSE} and the regularization factor λ are given as follows, respectively:

$$\beta_{\mathrm{MMSE}} = \sqrt{\frac{\mathrm{E_T}}{\mathrm{tr}\left(\left(\mathbf{H}^H\mathbf{H} + \lambda\mathbf{I}\right)^{-2}\mathbf{H}^H\mathbf{R}_{\mathrm{s}}\mathbf{H}\right)}}\,, \tag{3.12}$$

$$\lambda = \frac{\mathrm{tr}\left(\mathbf{R}_{\mathrm{n}}\right)}{\mathrm{E_T}}\,, \tag{3.13}$$

being $\mathbf{R}_{\mathrm{n}}$ defined as the noise covariance matrix:

$$\mathbf{R}_{\mathrm{n}} = \mathrm{E}\left[\mathbf{n}\mathbf{n}^H\right]\,. \tag{3.14}$$

When large transmit power can be used, the Lagrange multiplier λ is zero and the constraint in eq. (3.10) becomes inactive. In this case, it converges to the ZF filter. On the other hand, when the available transmit power is small the Lagrange multiplier reaches very a high value (tends to infinity) and the filter converges to an MF.

3.1.4 Block Diagonalization (BD)

The BD precoder consists of a transmit filter able to cancel all the multi-user interference. Its name owns to the fact that the product $\mathbf{HP}$ will be block diagonal unless no MIMO structures are applied where such a product would end up in a totally diagonal matrix. Since the diagonalization is done block-wise, the interference among streams of each user still remains and thus must be treated at the receiver side. When using this precoder, in this work, it is assumed that the receive processing $\mathbf{G}$ is implemented as a ZF filter.

In order to transmit streams intended to a certain MS without causing interference to the other MSs, it is sufficient to project such transmit streams onto the null space of $\tilde{\mathbf{H}}_{\mathrm{i}}$ - the joint channel $\tilde{\mathbf{H}}_{\mathrm{i}}$ regarding all the other MSs. Additionally to this block-wise ZF, an MF can be applied so as to boost the desired signal portion. The eq. (3.15) shows the transmit filter designed for the MS i.

$$\mathbf{P}_{\mathrm{BD,i}} = \mathbf{V}_{\mathrm{null}}(\mathbf{H}_{\mathrm{i}}\mathbf{V}_{\mathrm{null}})^H \in \mathbb{C}^{N_{\mathrm{T}}\times N_{\mathrm{r}}}\,, \tag{3.15}$$

where $\mathbf{V}_{\mathrm{null}} \in \mathbb{C}^{N_{\mathrm{r}}\times rank\left(\tilde{\mathbf{H}}_{\mathrm{i}}\right)}$ is a matrix whose colums form a basis to the null space of $\tilde{\mathbf{H}}_{\mathrm{i}}$; and $\mathbf{H}_{\mathrm{i}}$ is the channel regarding only MS i.

The unconstrained transmit power expression of the joint BD precoder can be finally conceived

by gathering all individual precoders in a single matrix as bellow.

$$\mathbf{P}_{\mathrm{BD}} = [\mathbf{P}_{\mathrm{BD},1} \quad \mathbf{P}_{\mathrm{BD},2} \ldots \mathbf{P}_{\mathrm{BD,K}}] \ . \tag{3.16}$$

3.1.5 Tomlinson-Harashima Precoder (THP)

The THP technique is a nonlinear technique that can be seen as the counterpart of the *decision feedback equalizer* at the receiver. In a THP system, the already transmitted symbols are fed back in a closed loop and *modulo operations*, which are denoted by $\mathrm{M}(^*)$, are applied at both transmitter and receiver, [**?**, 9, 10, 16]. The idea behind the THP theory is illustrated in Fig. 3.1.

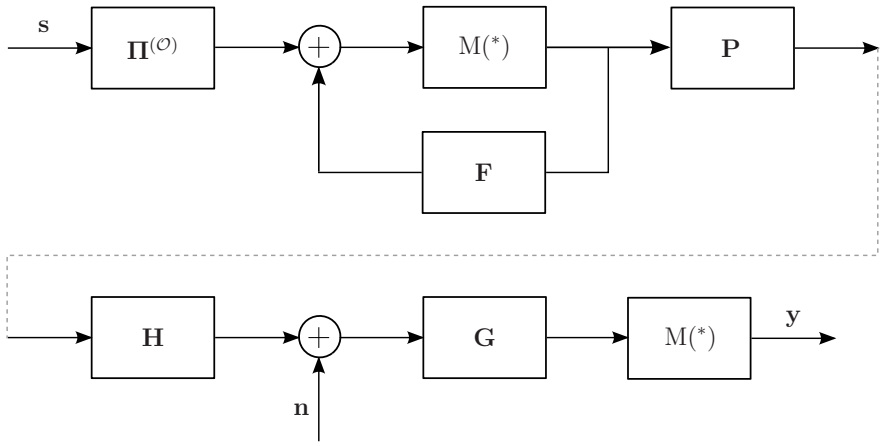

Figure 3.1: Block diagram of the THP transmission/reception chain.

The forward and feedback filters are given by

$$\mathbf{P} = \mathbf{H}^H \mathbf{\Pi}^{(\mathcal{O}),T} \mathbf{L}^{H,-1} \mathrm{diag}(l_{1,1}^{-1}, ..., l_{N_\mathrm{R},N_\mathrm{R}}^{-1}) \tag{3.17}$$

and

$$\mathbf{F} = \mathbf{I}_B - \mathbf{L}\,\mathrm{diag}(l_{1,1}^{-1}, ..., l_{N_\mathrm{R},N_\mathrm{R}}^{-1}) \,, \tag{3.18}$$

respectively. $\mathbf{L} \in \mathbb{C}^{N_\mathrm{R} \times N_\mathrm{R}}$ is obtained from the Cholesky decomposition of the channel Gram matrix $\mathbf{H}\mathbf{H}^H$, $l_{i,i}$ is an element of the main diagonal of $\mathbf{L}$, and the receive filter $\mathbf{G}$ is assumed to be a real scalar gain.

The $\mathbf{\Pi}^{(\mathcal{O})}$ matrix is responsible for permuting the symbols in such a way that the signal levels at the output of the THP system are maximized. The ordering process considered for the simulations in this work is described in [?, 12].

3.1.6 QR decomposition based Successive Interference Cancellation (QRSIC)

This is a nonlinear technique similar to THP in some sense. The basic difference between them is that QRSIC does not perform any ordering and no energy normalization is applied (the term $\mathrm{diag}(l_{1,1}^{-1}, ..., l_{N_\mathrm{R},N_\mathrm{R}}^{-1})$ in eq. (3.17) forces the energy to be distributed uniformly among all transmit symbols). In addition to that, a QR decomposition is used here rather than a Cholesky one as in THP. This technique is an implementation of the algorithm described in [15]. The forward and feedback filters of the QRSIC algorithm, respectively, are given by

$$\mathbf{P} = \mathbf{H}^H \mathbf{Q}^H \,, \tag{3.19}$$

$$\mathbf{F} = \eta \left(\mathbf{I} - \mathbf{R}^H \mathrm{diag}(r_{1,1}^{-1}, ..., r_{N_\mathrm{R},N_\mathrm{R}}^{-1})^{-1} \right) \,, \tag{3.20}$$

where $\mathbf{Q} \in \mathbb{C}^{N_\mathrm{R} \times N_\mathrm{R}}$ and $\mathbf{R} \in \mathbb{C}^{N_\mathrm{R} \times N_\mathrm{R}}$ are obtained from the QR decomposition of the channel Gram matrix, $r_{i,i}$ is an element of the main diagonal of $\mathbf{R}$, the receive filter $\mathbf{G}$ is assumed to be a real scalar gain, and η is a regularization parameter, which has a role equivalent to that of the λ parameter of the linear MMSE algorithm. The name QRSIC used here comes from the fact that the way it precancels interference at the transmitter resembles the multiuser detection technique called Successive Interference Cancelation (SIC) at the receiver and it makes use of a QR decomposition.

3.2 Performance Evaluation

In order to compare the performance of our linear and non-linear precoders a series of simulations has been carried out. The chosen scenario was a 3-cell cluster where perfect BS cooperation is allowed. As we have only one cluster without wrap-around all the interference can fully be treated by the joint transmitter formed by the 3 cooperative BSs inside the cluster.

Two antenna configurations have been investigated ($N_t \times N_r$) 1x1 and 2x2. Two channel models have been considered: with and without path-loss (in the latter case path-loss is set to a fixed value, MSs do not move across snapshots of the simulation and only fast-fading is snapshot-varying). The former is the classical one, whereas the latter is an ideal symmetric strong CCI scenario used to examine the performance of joint precoders under Rayleigh fading only and hence to reveal the achievable performance bounds for BS cooperation. The joint precoders were also evaluated under two different transmit power contraints: pooled and per-base power contraints.

Performance of joint precoders regarding only the MS that experimences the worst channel

was also assessed.

The output measurement used to evaluate the joint precoders is the *average spectral efficiency per user* $\mathbf{C}_{avg}$, given by eq. (3.21) as follows

$$\mathbf{C}_{avg} = \frac{1}{K} \sum_{i=1}^{N_r K} \log_2 \left(1 + \mathrm{SINR_i}\right). \tag{3.21}$$

The SINR measured at the i-*th* receive antenna element (regarding all MSs) in eq. (3.21) is given by eq. (3.22).

$$\mathrm{SINR_i} = \frac{|h_{ii}|^2}{\sum_{j \neq i} |h_{ij}|^2 + P_{noise}}, \tag{3.22}$$

where h_{ij} corresponds to the element located in the i-*th* row and j-*th* column of the equivalent channel $\mathbf{HT}$, and P_{noise} is the noise power.

The $\mathbf{C}_{avg}$ was obtained by varying the *average SNR per MS* Γ for the case with fixed path-loss, or the *average SNR measured at half the distance between BS and the cell border* Γ^* for the case with varying path-loss. The average SNR here is an input parameter consisting of a map from the transmit power which is also an input parameter in fact. So, one could be used instead of the other, however an average SNR was thought to be more suitable.

All precoders are also compared to the Sato's bound, which is the sum rate of a heuristic cooperative system where both transmitters and receivers can cooperate with each other [4]. It is given by [17]

$$\mathrm{SR}_{Sato} = \max_{\mathrm{tr}(\mathbf{TT}^H) \leqslant P_t} \log \frac{|\mathbf{\Phi}_n + \mathbf{HTT}^H \mathbf{H}^H|}{|\mathbf{\Phi}_n|}, \tag{3.23}$$

where $\mathbf{\Phi}_n$ is the noise covariance matrix. In order to plot the Sato's bound, the numerical method described in [18] was considered, which is based on the iterative water-filling algorithm.

The two investigated antenna schemes are: $(1, 1, 3, 3)$ and $(2, 2, 3, 3)$. For both, two different scenarios were evaluated: a realistic one considering per-base power constraints and all signal losses (path-loss, shadowing and Rayleigh fading are present) and an idealized one where all BSs are constrained by a pooled amount of transmit power and only Rayleigh fading is considered (fixed path-loss).

Figures 3.2 and 3.3 show the superiority of nonlinear precoders over the linear ones. The ZF is the simplest algorithm having the worst performance, as it wastes a larger portion of the available transmit power to invert the channel. The MMSE has a better performance over ZF, once it preserves more of the transmit power at the cost of allowing some interference to remain. This means that it does not perfectly diagonalize the channel as the ZF does. One can also see

that MMSE converges to the ZF for high values of SNR, which is an expected behavior, since the *regulation factor* in eq. (3.11) goes to zero as the SNR increases. MMSE also presents a better performance than both BD and ZF-THP for low SNR values. This behavior is due to the fact that these last two algorithms invert the channel without regularization. For higher SNR values, however, the advantage due to the regularization vanishes and MMSE is outperformed by BD and ZF-THP.

An interesting point in Fig. 3.2 is that BD meets ZF in performance, which is an expected result from theory (a block-diagonalization with blocks of dimension $1\text{x}1$ is merely an ordinary diagonalization like the ZF approach). On the other hand, regardless of the assumption of some processing at the receiver, BD can outperform the linear precoders when more than one antenna is present in both BS and MS and reasonable CSI is available at the receiver side. It saves power by not totally diagonalizing the channel - instead, it makes use of null-space decompositions (explained in **??**) to block-diagonalize the joint channel and hence to avoid interference among cochannel MSs. Owing to the fact that interference among symbols of the same user still remains in the equivalent channel (channel transformed by precoder), receiver processing is thus required to complete the interference cancelation task. In our simulations, the variant of BD that uses a matched filter (see eq. (**??**)), instead of a projection onto the signal space of the *virtual channel*, is used to concentrate more power in the diagonal elements of the equivalent channel.

In Figs. 3.2(b) and 3.3(b) the ZF-THP gets closer to QRSIC in the idealized scenario. The reason for this is that a global power constraint is assumed for the idealized scenario, and this implementation of THP extracts better performance using this kind of power constraint when compared to the case where per-base power contraints are considered (realistic scenario).

The Fig. 3.4 show how the average spectral efficiency of the $2\text{x}2$ schemes evaluated in this chapter is distributed for a fixed average SNR value, in this case 10dB. The 50th percentile roughly reflects the average spectral efficiency presented in Fig. 3.3 for a 10dB SNR value.

The analysis of the 90th percentile, which indicates that only 10% of the users are capable of achieving a spectral efficiency higher than the x-axis value, reveals that the QRSIC algorithm achieves a much higher peak rate than the other ones. It is also seen that ZF and MMSE tend to converge to each other. The same convergence is observed between BD and THP in Fig. 3.4(a).

At the 10th percentile, however, QRSIC has a performance comparable to the other algorithms, and is even surpassed by THP in the idealized scenario. The reason for this performance degradation is discussed in the end of this section. The curve-crossing behavior of MMSE can also be verified in the figures, being more pronounced for the realistic scenario, in which it provides roughly the same performance as QRSIC.

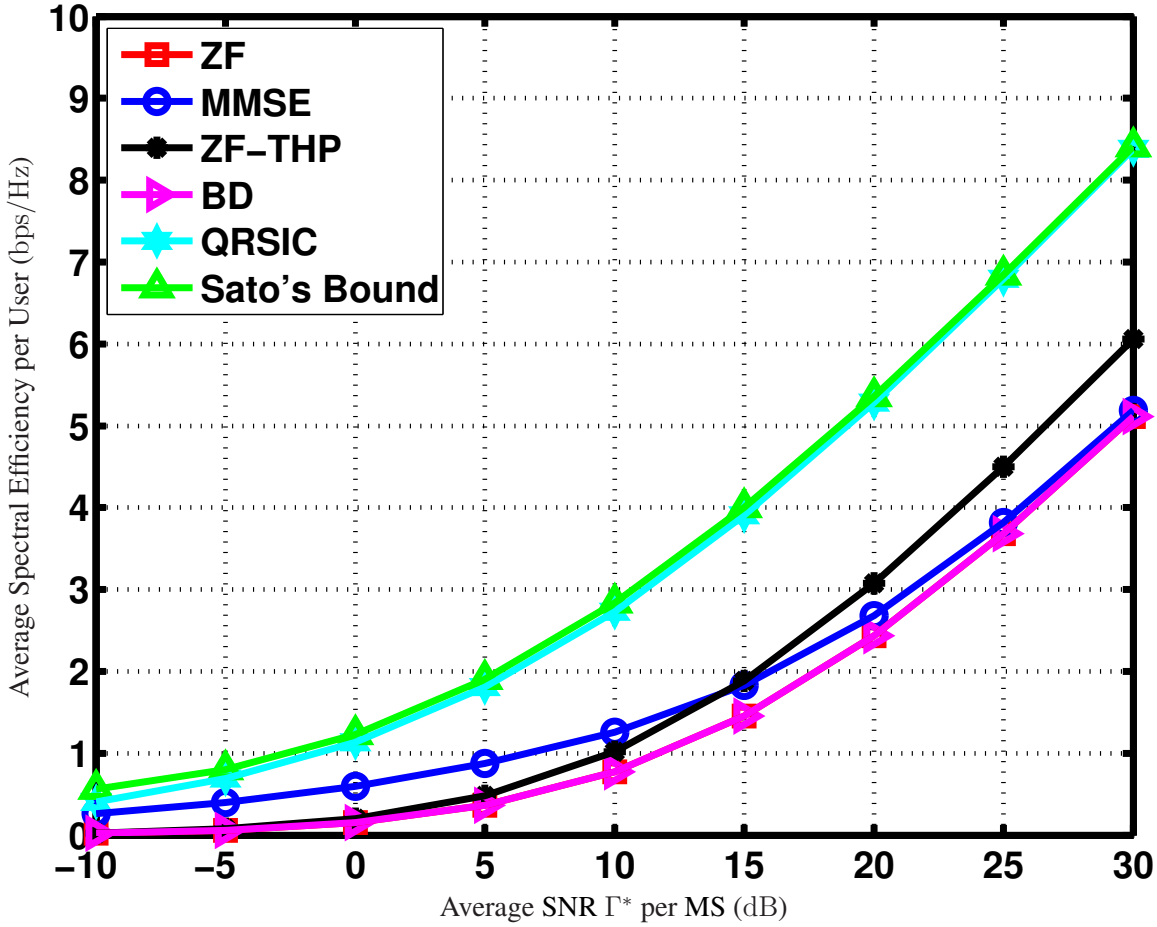

(a) Performance curves for a realistic scenario using per-base power constraints in a 1x1 scheme. The Γ^* means an average SNR at half the distance between BS and cell border.

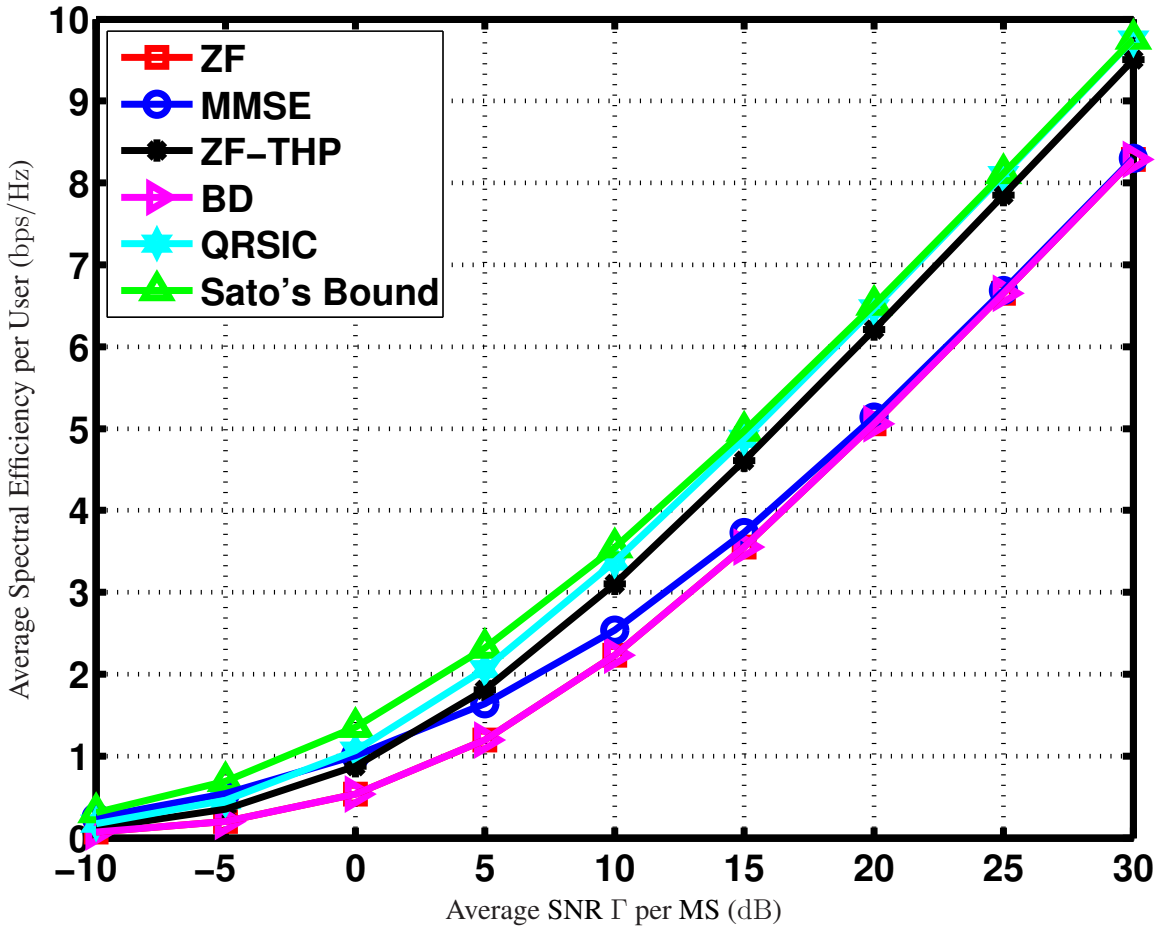

(b) Performance curves for a idealized scenario using global power constraint in a 1x1 scheme.

Figure 3.2: Performance curves in a 1x1 scheme

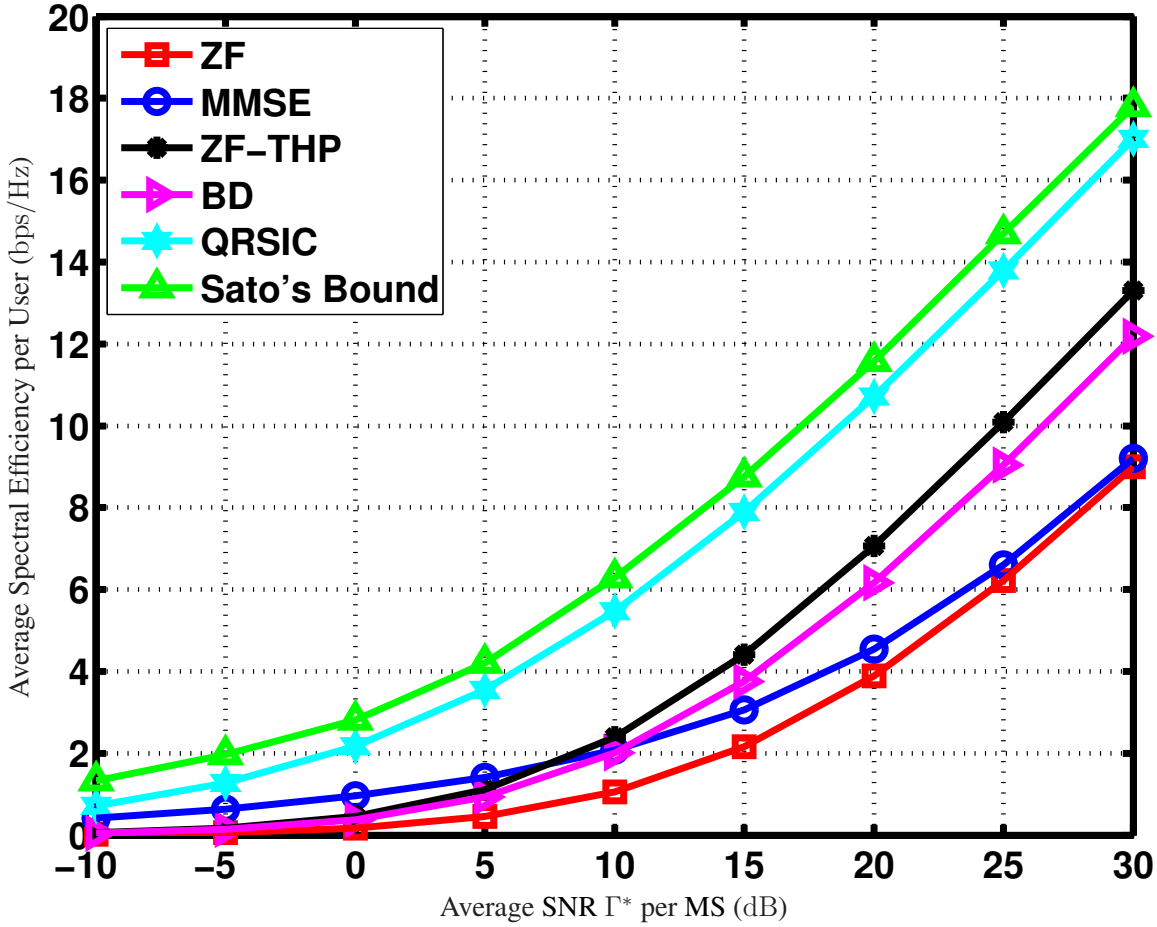

(a) Performance curves for a realistic scenario using per-base power constraints in a 2x2 scheme. The Γ^* means an average SNR at half the distance between BS and cell border.

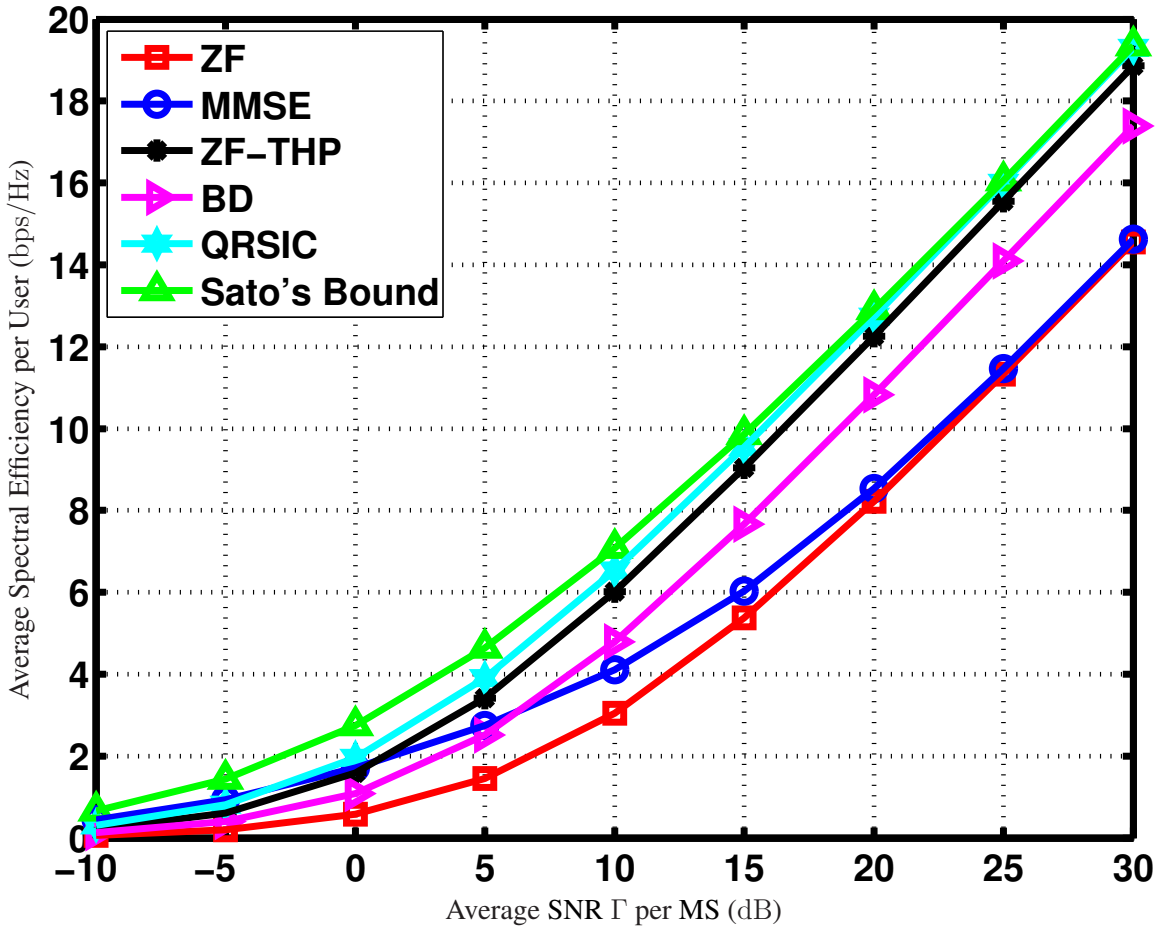

(b) Performance curves for a idealized scenario using global power constraint in a 2x2 scheme.

Figure 3.3: Performance curves in a 2x2 scheme

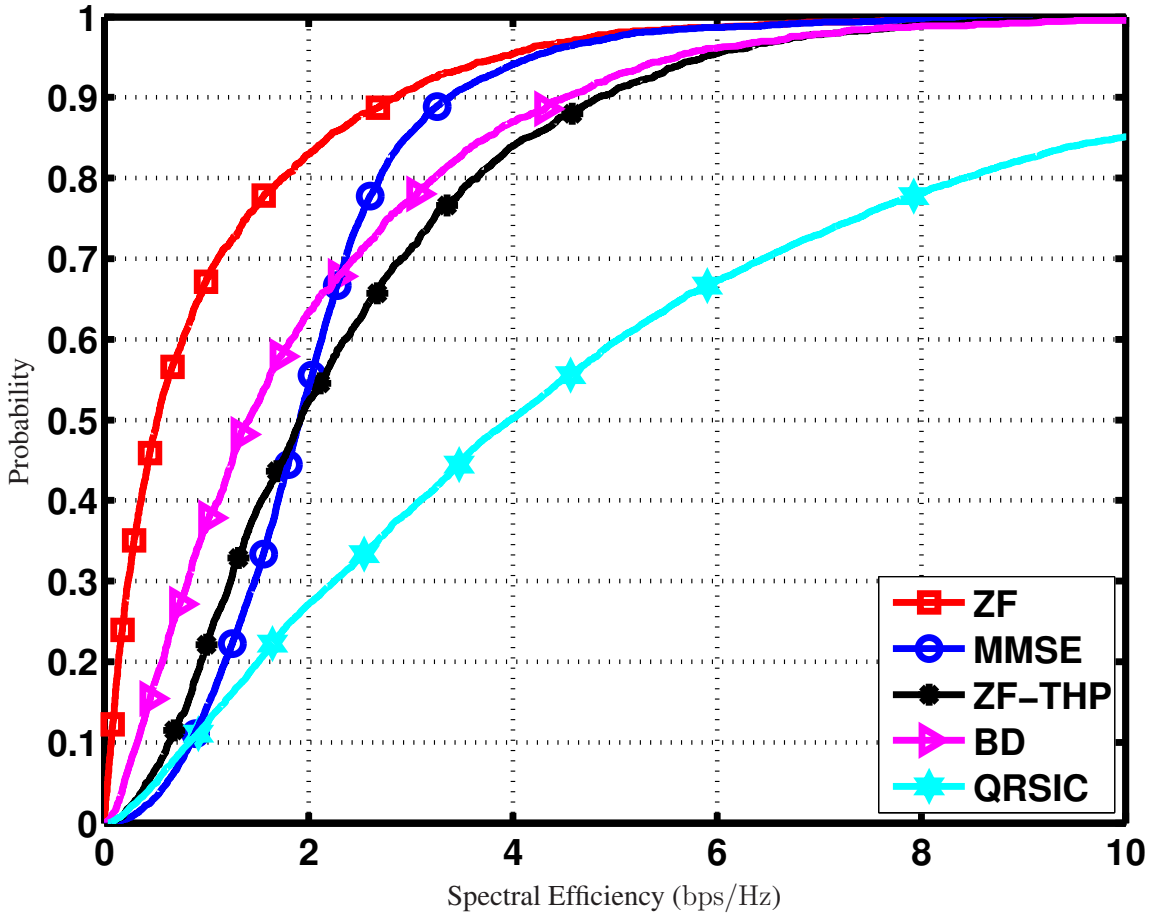

(a) CDF curves for a realistic scenario using per-base power constraints in a 2x2 scheme for an average SNR at half distance between BS and cell border (Γ^*) of 10dB

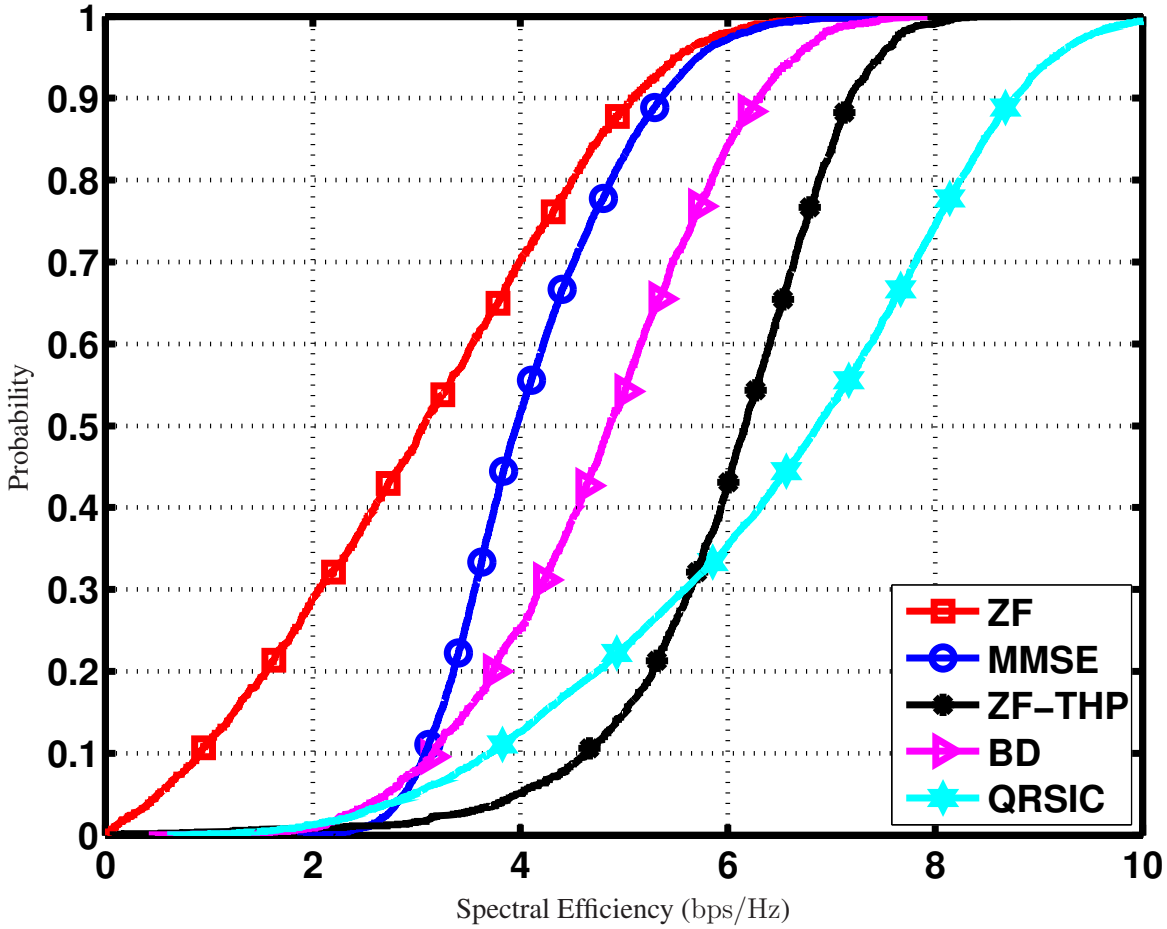

(b) CDF curves for a idealized scenario using global power constraint in a 2x2 scheme for an average SNR per user (Γ) of 10dB.

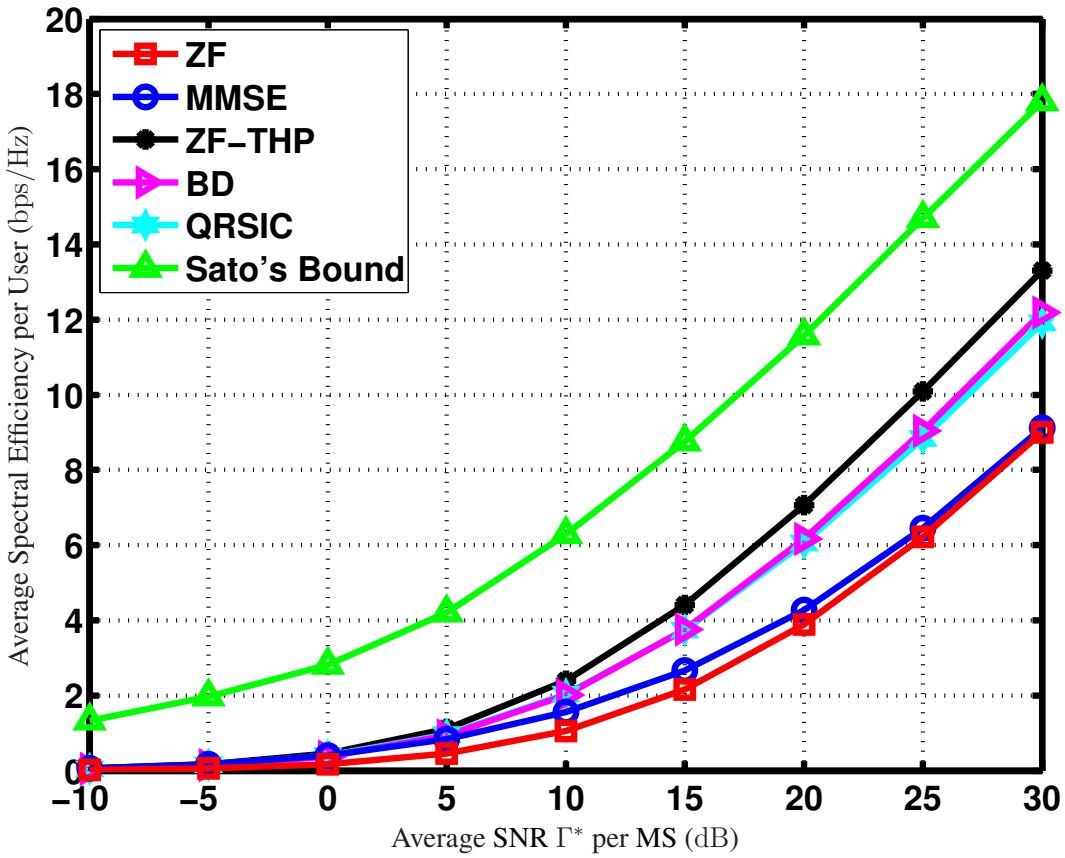

Figure 3.5: Performance curves considering the worst user in a realistic scenario using per-base power constraints in a 2x2 scheme. The Γ^* means an average SNR at half the distance between BS and cell border

The results so far showed an average behavior of each precoder algorithm. The object of investigation in this part is to see how constant they keep rates among all MSs, i.e., how much they differ from their average behavior to the case of the MS with worst channel conditions. From figure 3.5 it is clear that all algorithms except QRSIC and MMSE present a worst-MS performance almost equal to the average-MS one, i.e., all MSs are assured the roughly same quality. The MMSE should not be grouped in this category together with QRSIC, as it shows just a minor oscillation from the average case to the worst one. On the other hand, QRSIC presents a strong oscillation, which shows that it is a suitable technique for maximizing the average sum rate per MS at the cost of allowing such variations in keeping rates among MSs. The other precoders can handle well this task because they force MSs to get the same rates. From this point of view, THP outperforms QRSIC (the opposite occurs for the average case), since it is able to provide a higher worst-MS rate. This is similar to what is observed at the 10th percentile of figure 3.4(a).

3.3 Error Sensitivity Evaluation

The purpose of this section is to evaluate *joint precoding* in a multicell multiuser MIMO system where perfect base station cooperation is assumed. Differently from the previous analysis done in [4], where perfect CSI at the transmitter was considered, this section intends to evaluate the performance of precoding techniques for different levels of channel estimation error, thus better modeling realistic scenarios. For reaching such an aim, both the performance (measured as the average spectral efficiency per user) and the *error sensitivity* of each precoder have been analyzed.

The evaluation done in this section follows the model presented in chapter 2 but assuming that at the transmitter side only an estimate $\hat{\mathbf{H}} \in \mathbb{C}^{N_{\mathrm{R}} \times N_{\mathrm{T}}}$ of the actual channel matrix $\mathbf{H}$ is available. The matrix $\hat{\mathbf{H}}$ is modeled here as being the sum of the exact joint channel matrix $\mathbf{H}$ (whose entries take into account path-loss, shadowing and zero mean unit variance fast-fading combined) and a perturbation matrix $\mathbf{E}_{\mathrm{T}}$ with Gaussian distributed entries, which have the same mean value as those in $\mathbf{H}$ (due to path-loss and shadowing) and a variance σ_e^2, i.e.,

$$\hat{\mathbf{H}} = \mathbf{H} + \mathbf{E}_{\mathrm{T}} \,. \tag{3.24}$$

So, the available channel for the precoding design is the estimated one in (3.24) instead of the exact one in (2.1).

At the receiver side, depending on the considered receive processing algorithm, an estimate $\hat{\mathbf{H}}_{\text{eq}} \in \mathbb{C}^{N_{\mathrm{R}} \times N_{\mathrm{R}}}$ of the equivalent channel $\mathbf{H}_{\text{eq}} = \mathbf{HT} \in \mathbb{C}^{N_{\mathrm{R}} \times N_{\mathrm{R}}}$ may also be required. Since the focus of this evaluation is on the processing done at the transmitter side only, perfect channel knowledge at the receivers is assumed, i.e., $\hat{\mathbf{H}}_{\text{eq}} = \mathbf{H}_{\text{eq}}$.

Let $(N_{\mathrm{t}}, N_{\mathrm{r}}, N_{\mathrm{b}}, N_{\mathrm{u}})$ indicate a scenario with N_{b} BSs equipped with N_{t} transmit antennas each and N_{u} MSs with N_{r} receive antennas each. Here, a scenario with two different antenna configurations, $(2, 2, 3, 3)$ and $(4, 2, 3, 3)$, is considered. The two receive antennas at each MS considered in the present simulations are assumed to be cross-polarized.

Each of the N_{b} cooperative BSs is placed in the center of a hexagonal cell with radius of $1000\mathrm{m}$. For each channel realization, one user is arbitrarily located in each cell. Rayleigh fading is assumed for small-scale fading. For the large-scale fading, shadow fading is simulated with a variance of $\sigma^2 = 6\mathrm{dB}$ and the following path-loss expression is employed:

$$G_{\mathrm{PL}} = 15.3 + 37.6 \log_2 d \qquad [\mathrm{dB}] \,, \tag{3.25}$$

where d is the distance between BS and MS.

Simulations are performed for a low and a high average SNR (at cell edge), namely $-5\mathrm{dB}$ and $20\mathrm{dB}$, along with different values for the perturbation variance σ_e^2 varying from $-40\mathrm{dB}$ (negligible perturbation, and thus considered here as the absence of channel estimation error) to $10\mathrm{dB}$ (actually this corresponds to an impractical channel error, but is considered so as to visualize the tendency of curves in the graphical results).

The present performance analysis is twofold: an absolute performance evaluation and an error sensitivity evaluation. The former is intended to measure the impact of different antenna configurations on the average spectral efficiency per user (in $\mathrm{bps/Hz}$) of each precoder assuming a $20\mathrm{dB}$ average SNR at the cell edge in the presence of an unreliable channel estimation, whereas the latter focuses on how much each precoder has its performance diminished as the channel estimation error grows, i.e., how resistant they are against fluctuations in channel estimation assuming low and high values for the average SNR at the cell edge.

Figs. 3.6(a) and 3.6(b) show the performance of the precoders for two different antenna configurations assuming imperfect channel estimation for different values of perturbation. When comparing both figures, we can see that the linear technique ZF has its performance scaled by N_t for negligible perturbation. The same happens to MMSE, due to the convergence to ZF for high SNR. Although block-diagonalization-based precoding is also a linear processing technique, it does not follow the same behavior as ZF and MMSE concerning the antenna configuration, as it does not decouple the MIMO channels for each BS-MS pair into parallel interference-free subchannels (or near interference-free in the case of MMSE). On the other hand, the BD technique has better performance compared to the other linear techniques. These results also show that this precoder can also outperform nonlinear techniques in the presence of harmful channel perturbation. Another interesting outcome of these results is that, apart from the BD precoder, all the others converge to a common performance for strong channel estimation errors, which implies that under such a harmful perturbation in channel estimation there is no improvement on the increase of antennas in the MIMO structure. For such high error variances, diversity techniques, which do not depend on the quality of the channel estimation, should be preferred.

Figs. 3.7(a) and 3.7(b) show the behavior of each precoder regarding their sensitivity to estimation errors for both low and high SNR values and a $(4, 2, 3, 3)$ antenna configuration. The sensitivity to estimation errors $\Psi(\sigma_\mathrm{e}^2)$ is defined as the ratio of the average spectral efficiency per user given a certain error variance $S(\sigma_\mathrm{e}^2)$ to the average spectral efficiency per user of the error-free case S_0, i.e.,

$$\Psi(\sigma_\mathrm{e}^2) = 10\log_{10}\left\{\frac{S(\sigma_\mathrm{e}^2)}{S_0}\right\} \qquad [\mathrm{dB}]\,. \tag{3.26}$$

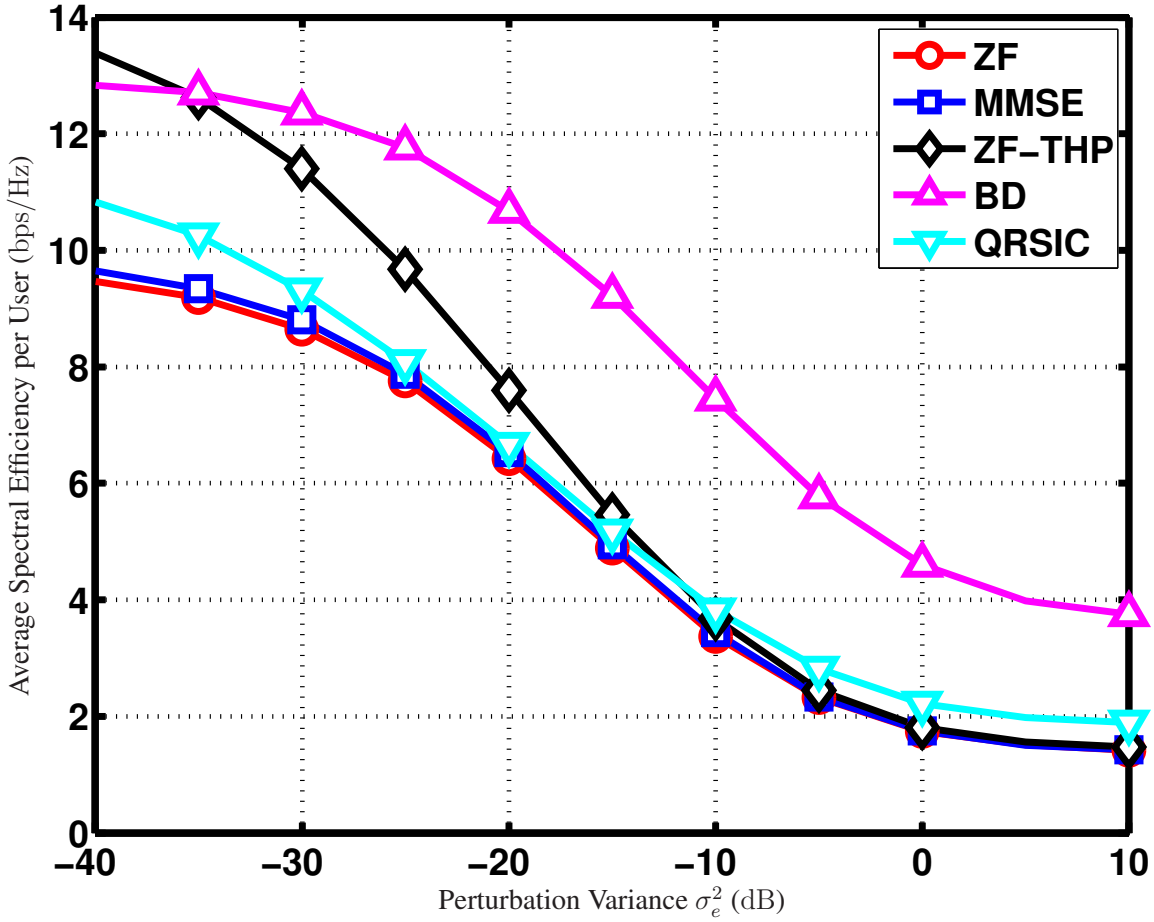

(a) $(2, 2, 3, 3)$ case.

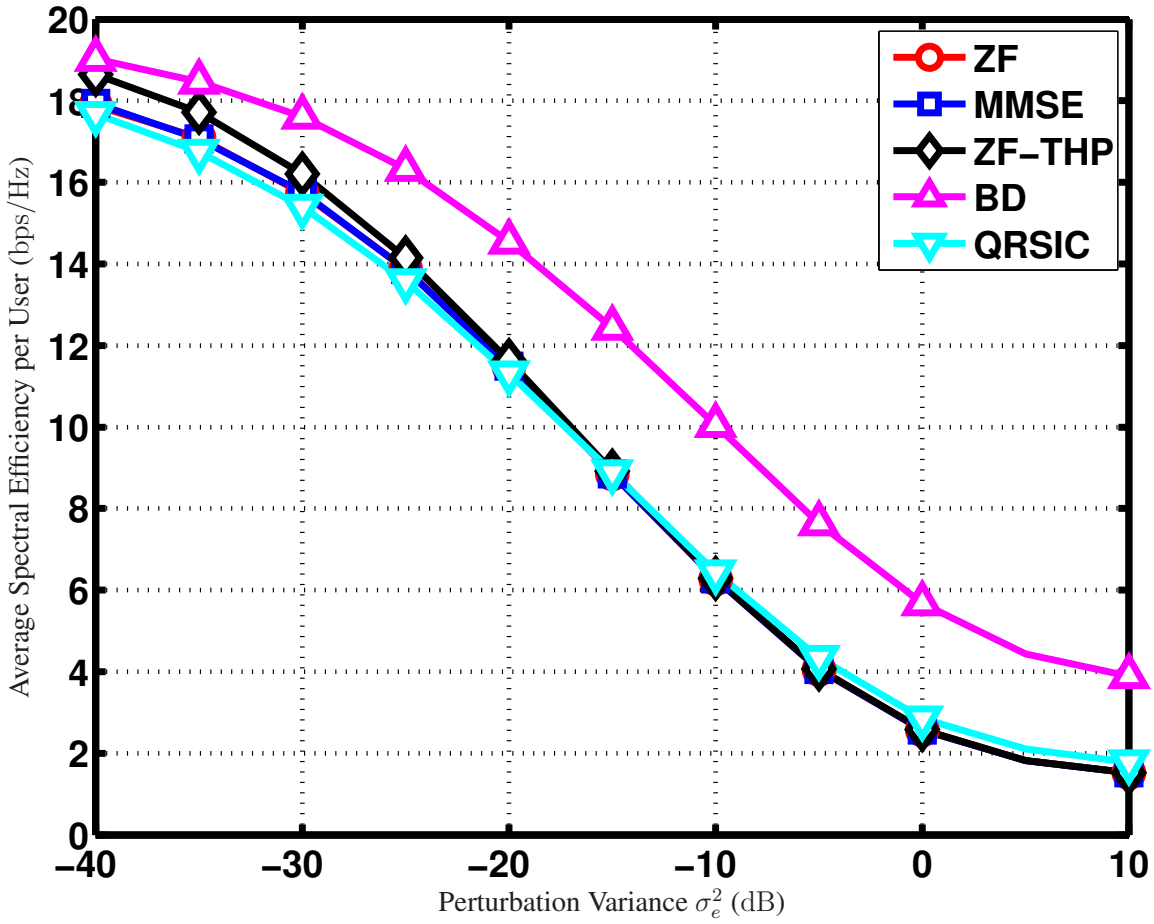

(b) $(4, 2, 3, 3)$ case.

Figure 3.6: Performance Curves for a 20dB **average SNR at the cell edge and different antenna configurations.**

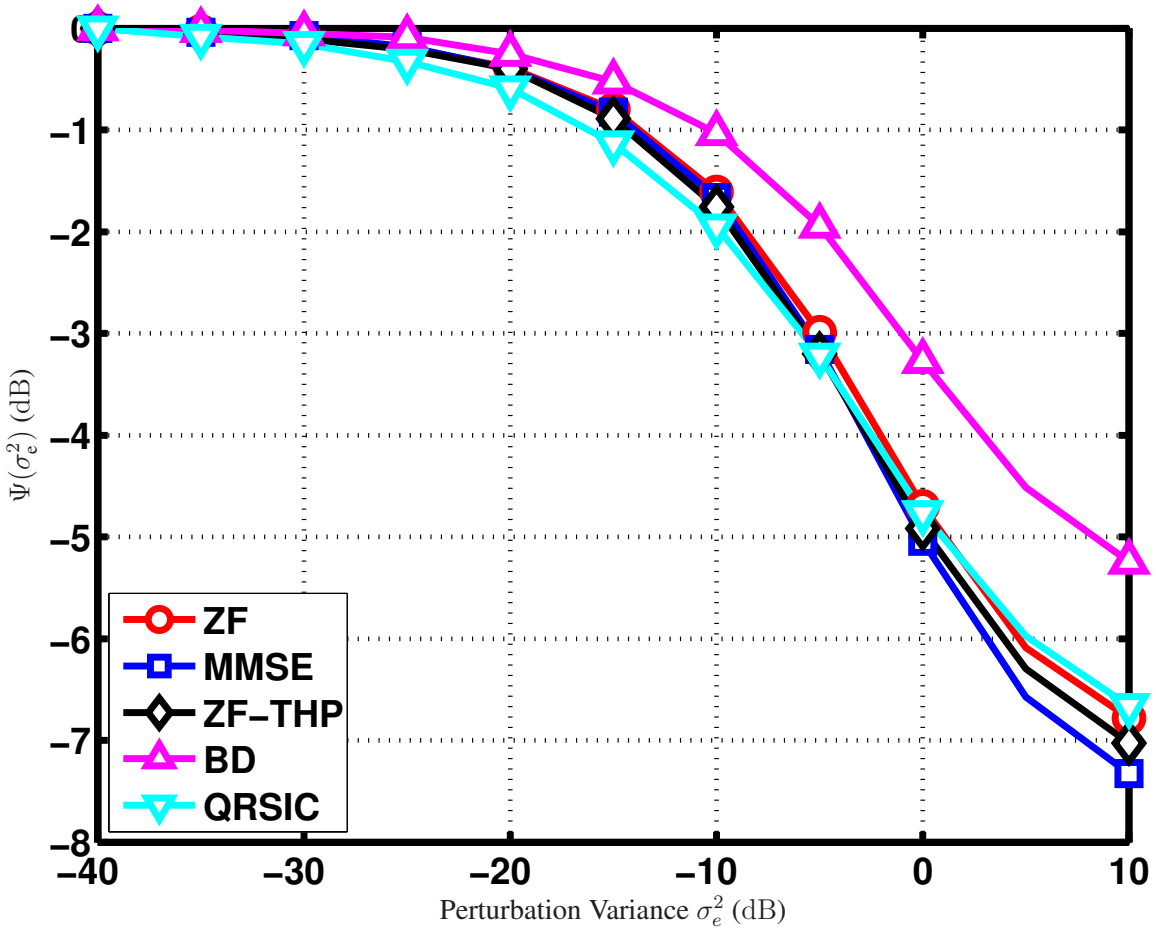

(a) -5dB average SNR at the cell edge.

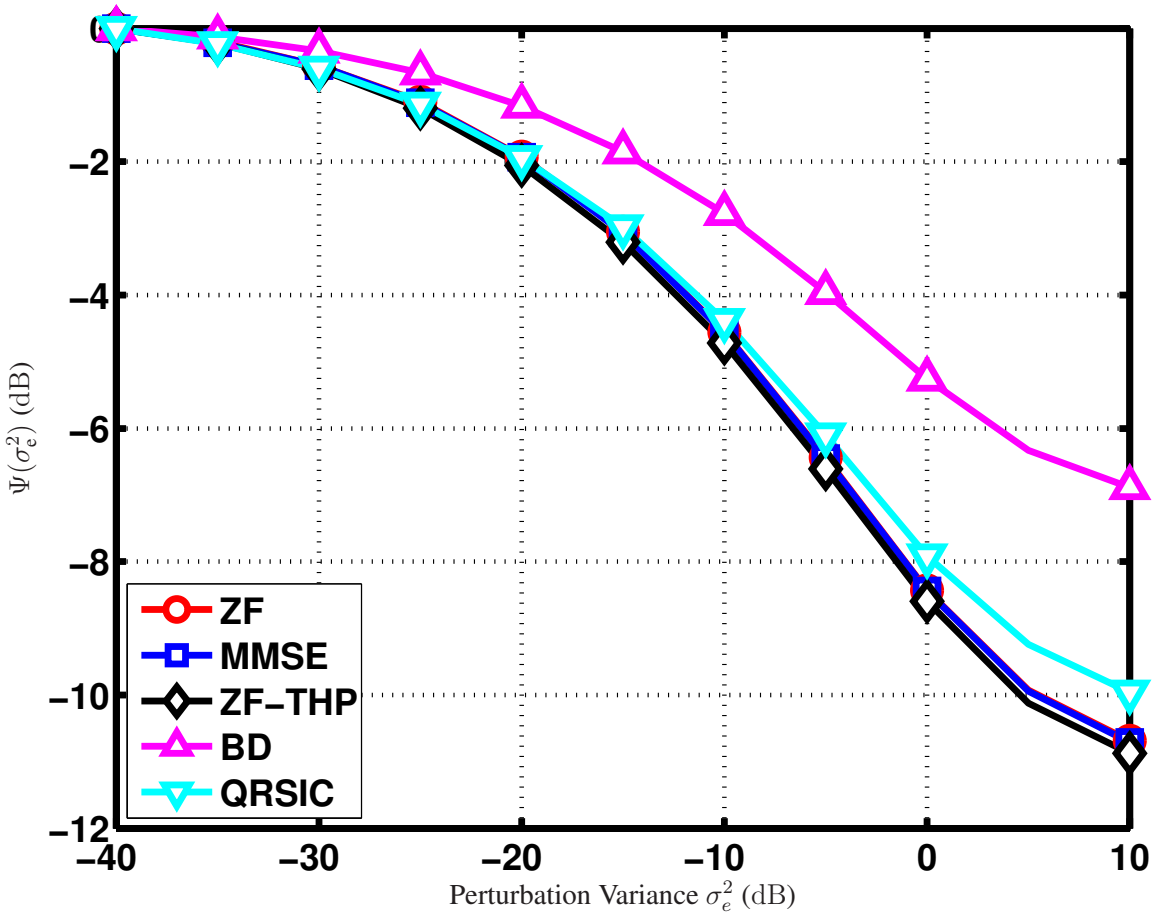

(b) 20dB average SNR at the cell edge.

Figure 3.7: Sensitivity Analysis for the $(4, 2, 3, 3)$ case and different SNR values at the cell edge.

These results reveal that the BD precoder is the least sensitive in this sense and that all the other precoders seem to behave similarly.

In spite of the apparent advantage of the BD technique over all the other algorithms in terms of error sensitivity, there are some other relevant issues that need to be discussed. Firstly, the BD requires a higher receiver complexity, since the interference among streams of a same user needs to be mitigated at the receiver. Secondly, it has been assumed in the simulations that no estimation errors were made at the receivers. It is therefore expected that, if estimation errors at the receiver are of the same order as those at the transmitter, then the BD algorithm should present a behavior similar to that of the other techniques. For these reasons, the BD algorithm would be more advisable for situations in which the channel estimation at the receivers presents a good reliability.

Chapter 4

Precoding-Aware Inter-Cell Scheduling - A Combined Approach

In the previous chapter 3 joint precoding techniques were shown to be a valid approach in interference management in a cooperative scenario with just one cluster. When more than one cluster is considered, another type of interference arises – the *out-of-cluster interference* – which is taken into account in this chapter. As no cooperation among clusters is assumed, the out-of-cluster interference cannot be cancelled.

In addition to precoding techniques, there are other techniques commonly labeled as scheduling techniques that differently from precoding ones they do not pre-cancel interference at transmitter side but try to avoid it, thus reducing interference levels and enhancing SINR. Complete knowledge of MSs's channel gains, as in precoding discussion, is assumed to be available at the transmitter side. Additionally, BS scheduling demands a cooperation between the BSs involved. Regardless some SINR enhancement, by turning some BSs inactive a spectral efficiency loss is expected, which does not occur when using only precoding where all BSs are kept active and energy is spent to separate MSs within a cluster. By turning some BSs to be inactive SINR values are improved at the cost of spectral efficiency loss. A perfect trade-off between reasonable SINR values and spectral efficiency loss is hard to be reached.

A natural step further in tis issue would be a combination of the two techniques, precoding and scheduling, in order to take advantage of gains provided by both of them. Such a combination is explored twofold in this chapter: a bare combination – which consists of applying a BS scheduling algorithm to avoid a certain amount of interference like those in section 4.1 followed by a precoding techinque to cancel the residual interference; and a much smarter combination (our proposal) – which intends to perform just either a BS scheduling alone or allow all cooperative BSs to be

active, perform a MS scheduling and apply a joint precoding afterwards to those scheduled MSs in a iterative way where the MS scheduling is done according to current achieved rates after precoding application, so as to maximize the cluster sum spectral efficiency.

4.1 Inter-Cell Scheduling

In this section the basics of some BS scheduling algorithms are described. For all algorithms presented in this section it is assumed that the MS with the best channel conditions in every cooperative cell of the cluster has been already scheduled (this omited task is a MS intra-cell scheduling) before any BS scheduling takes place. It is assumed that each MS is served by the BS he is assigned to, and for the sake of simplicity each pair BS-MS is located in the same cell.

A further discussion about the BS scheduling algorithms in this section can be found in [1].

4.1.1 Simultaneous Transmission (ST)

The ST algorithm consists of keeping all cooperative BSs active within the cluster, i. e. no BS scheduling is actually done.

4.1.2 Orthogonal Inter-Cell Scheduler (OIS)

The OIS algorithm consists of keeping active only the BS whose cell reside the MS with the best channel conditions regarding the entire cluster. This technique presents the worst spectral efficiency loss due to the inactive BSs (the larger cluster the larger spectral efficiency loss), but offers the best SINR levels once all interference within the cluster has been avoided.

4.1.3 Non-Orthogonal Inter-Cell Scheduler (NOIS)

The NOIS algorithm searches for the best combination of active and inactive BSs that maximizes the cluster sum spectral efficiency.

4.2 Inter-Cell Scheduling and Precoding Combined

Through BS cooperation each cooperative BS equipped with one antenna, at least, may contribute to a *virtual MIMO* structure between transmitter and receiver assuming that this last might be equipped with more than one antenna element as considered in chapter 3 in spite of the multiple-antenna size limitation issue on mobile phones. However, in our work due to some

pending features to be implemented, only one antenna element was considered for each end (BS and MS) in the simulations of this chapter.

Assuming then, a scenario where inside each cluster perfect BS cooperation is allowed and a virtual MIMO is thus feasible joint precoding can be applied after a scheduling algorithm, like those in section 4.1, has been run. This joint precoding is hence performed by the BSs which remained active in the BS scheduling procedure. All current scheduled MSs in a cluster (due to the intra-cell MS scheduling preceding the inter-cell BS scheduling) are now, differently from the case in section 4.1, served by all active BSs within the cluster. There are several possible combinations regarding the choice of scheduling and precoding algorithms to be used.

Note that when the chosen scheduler is the OIS there is no need of interference cancellation withing the cluster (the out-of-cluster interference still remains), once all the the other cooperative BSs that would generate interference are inactive. In our simulations, a MF is applied after OIS for SINR improvement. When ST is chosen as scheduler, in this scheme, any precoder works well, but no impact on the cluster spectral efficiency is seen regarding BS scheduling followed by precoding as all cooperative BSs remain active. On the other hand, the application of NOIS followed by any precoder turns out to actually explore BS scheduling and interference cancellation to the scheduled MSs through the available virtual MIMO structure.

4.3 Precoding-Aware Non-Orthogonal Inter-Cell Scheduler (PANOIS)

The idea of this section is to present an algorithm, namely PANOIS, that is a core part of IAPANOIS, which intends to be a step further from this one.

The PANOIS algorithm relies on the idea of applying precoding to smartly scheduled MSs. It assumes that all BSs are always active and its search for the best MSs to be scheduled is not an exhaustive one as in NOIS. Instead, it uses heuristic search algorithms like First Fit First (FFF) or Best Fit First (BFF) [19] to reduce complexity and offer reasonable results. The whole procedure is explained as follows.

Let $\mathcal{G}$ denote the set of all MSs within a cooperation group and $\mathcal{G}_\mathrm{s} \subset \mathcal{G}$ denote the set of scheduled MSs. The elements of these sets actually correspond to the MS indices, which can assume values between 1 and the number of users N_u. Let also the Outer Interference to Inner

Interference Ratio (OIR) to be defined as

$$\mathrm{OIR} = \frac{P_{oi}}{P_{ii}} \tag{4.1}$$

where P_{oi} is the total power received from outside the cluster and P_{ii} is that one inside the cluster.

The PANOIS algorithm iteratively tries to solve the optimization problem given below:

$$\mathcal{G}_\mathrm{s} = \underset{\mathcal{G}_\mathrm{s}}{\operatorname{argmax}} \log_2 \det\left(\mathbf{I} + \mathbf{H}_\mathrm{s}\mathbf{R}_\mathrm{s}\mathbf{H}_\mathrm{s}^H\right) \quad \text{s.t.} \quad \begin{cases} \mathrm{tr}\{\mathbf{R}_\mathrm{s}\} \leq \sum_{i=1}^{N_\mathrm{b}} P_i \\ \mathrm{OIR} < 1 \end{cases}, \tag{4.2}$$

where $\mathbf{H}_\mathrm{s}$ is the overall MIMO channel regarding the scheduled MSs belonging to $\mathcal{G}_\mathrm{s}$, P_i is the power constraint regarding the i^{th} BS, N_b is the number of BSs inside a cluster, and $\mathbf{R}_\mathrm{s}$ is the input covariance matrix given by

$$\mathbf{R}_\mathrm{s} = \mathrm{E}\{\mathbf{T}_\mathrm{s}\mathbf{s}_\mathrm{s}\mathbf{s}_\mathrm{s}^H\mathbf{T}_\mathrm{s}^H\}, \tag{4.3}$$

where $\mathbf{T}_\mathrm{s}$ is the precoding matrix calculated based on $\mathbf{H}_\mathrm{s}$ and $\mathbf{s}_\mathrm{s}$ is the symbol vector of the scheduled MSs. The PANOIS algorithm provides a suboptimal solution as it does not perform an exhaustive search (in order to drastically reduce complexity), although, as will be shown in Section 4.5, it offers better results than simply applying precoding after scheduling without any kind of awareness between the two procedures.

PANOIS chooses the first scheduled MS as the one capable of achieving the highest rates, i.e., the one presenting the highest channel gains with regard to its nearest BS. After that it searches for the next MS in a way depending on the chosen heuristic search algorithm (FFF or BFF) and according to a certain criterion. In this work, such a criterion is to improve the sum capacity within the cooperation group.

In each iteration of this procedure a certain precoding scheme is applied to the already scheduled MSs along with that one being tested so as to decide whether the tested MS is worthy of remaining scheduled or not, depending on the gain this addition offers to the sum capacity within the cluster. The feedback from precoder output to scheduler's next iteration is illustrated as a closed loop in Fig. 4.1. This algorithm provides a suboptimal solution to the scheduling problem of selecting the group of MSs that maximizes the sum capacity inside the cooperation group for the current precoding choice.

A more detailed description of the PANOIS algorithm is presented in Tables 4.1 and 4.2. It has

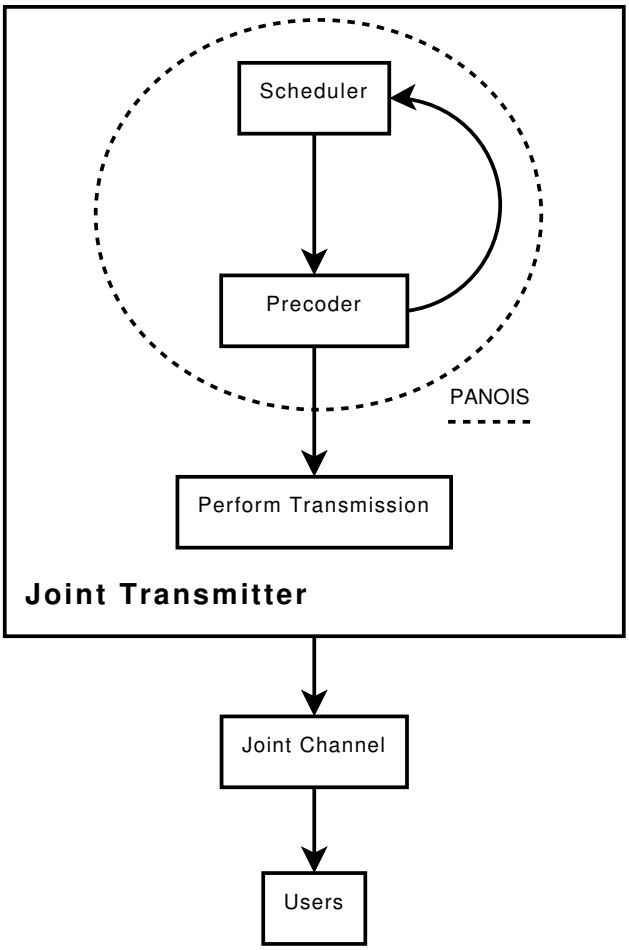

Figure 4.1: PANOIS block diagram

been assumed that $\mathbf{H}_i$ denotes the matrix of channel coefficients between MS i and its nearest BS, and $\mathcal{G}\{k\}$ denotes the k^{th} element of an ordered set.

The implementation of the FFF algorithm used in this work consists of a search that evaluates the gain in the sum capacity provided by the insertion of the current MS in test without going back (a MS tested will not be tested any longer) and goes into the next step as soon as a combination of MSs "fits" a selected criterion as the name of the algorithm implies. The next step works as the previous one, but the set of MSs does not include those who failed in the previous step. The BFF algorithm considered here has the same aim as FFF, searching in each iteration an MS that can improve the sum capacity that can be achieved with the current scheduled MS's. The difference from FFF is that BFF does not stop at the first time the current combination fits the criterion, instead it may go back to catch some past combination that could improve the sum capacity.

Table 4.1: Pseudo-code of PANOIS algorithm based on FFF.

$\mathcal{G}_{\mathrm{s}}^{\star} = \left\{ \underset{i \in \mathcal{G}}{\operatorname{argmax}} \lvert\lvert \mathbf{H}_i \rvert\rvert_{\mathrm{F}}^2 \right\};$	*Select first user*
$C_{\mathrm{s}}^{\star} = \log_2 \det \left(\mathbf{I} + \mathbf{H}_{\mathrm{s}}^{\star} \mathbf{R}_{\mathrm{s}}^{\star} \mathbf{H}_{\mathrm{s}}^{\star,H} \right);$	*Estimate capacity*
$\mathcal{G}_{\mathrm{ns}} = \mathcal{G} \setminus \mathcal{G}_{\mathrm{s}}^{\star};$	*Set with all other users*
$k = 1;$	
While $\lvert \mathcal{G}_{\mathrm{s}}^{\star} \rvert \leq N_{\mathrm{T}}/N_{\mathrm{r}}$ and $k < N_{\mathrm{u}}$, **do**:	
$\mathcal{G}_{\mathrm{s}} = \mathcal{G}_{\mathrm{ns}}\{k\} \cup \mathcal{G}_{\mathrm{s}}^{\star};$	*Test set with added user*
$C_{\mathrm{s}} = \log_2 \det \left(\mathbf{I} + \mathbf{H}_{\mathrm{s}} \mathbf{R}_{\mathrm{s}} \mathbf{H}_{\mathrm{s}}^{H} \right);$	*Estimate new capacity*
If $C_{\mathrm{s}} > C_{\mathrm{s}}^{\star}$,	*If rate improves*
$\mathcal{G}_{\mathrm{s}}^{\star} = \mathcal{G}_{\mathrm{s}};$	*Scheduled group update*
$C_{\mathrm{s}}^{\star} = C_{\mathrm{s}};$	*Capacity update*
end-if	
$k = k + 1;$	
end-while	

4.3.1 Complexity of the search methods

It is important to show how much the search done by PANOIS can drastically reduce complexity compared to the classical exhaustive search done in NOIS. Table 4.3 shows the complexity of each search method inside the cooperation group. Note that for the NOIS algorithm L represents the number of BSs per cooperation group, while for the FFF and BFF implementations used in PANOIS algorithm L refers to the total number of MSs within each cluster.

From Table 4.3 it can be seen that FFF has a linear complexity, whereas BFF has a quadratic one. Both are quite simple compared to the exponential complexity of the exhaustive search method, which might take significantly longer to be accomplished.

4.4 Interference-Adaptive Precoding-Aware Non-Orthogonal Inter-Cell Scheduler (IAPANOIS)

The IAPANOIS is, in fact, a variant form of PANOIS and is an algorithm capable of switching between pure BS-scheduling (NOIS and no precoding) to PANOIS depending on the OIR, which

is defined as

$$\mathrm{OIR} = \frac{P_{\mathrm{oi}}}{P_{\mathrm{ii}}} \tag{4.4}$$

where P_{oi} is the total power received from outside the cluster and P_{ii} is that one inside the cluster.

The motivation of this algorithm is that, in some cases, the out-of-cluster interference is found to be higher than that one within. In such cases, where this external interference is dominant, it is not beneficial to apply precoding, since the precoding will only be able to reduce the minor portion of the total interference generated inside the cluster leading to lower SINR values due to weaker transmit signals (after a significant amount of energy has been spent to cancel interference inside the cluster) and remaining significant interference.

For different cluster sizes a rough picture of the interference dominance is ilustrated in Fig. 4.2, regarding only distance-based path loss and interference from the immediately adjacent cells. Two regions are highlighted within each cluster, the outer region with $\mathrm{OIR} > 1$ and the inner with $\mathrm{OIR} < 1$. For small clusters the region dominated by P_{oi} might represent more than 70% of the cluster area, decreasing to roughly 30% for the depicted 12-cell cluster.

Table 4.2: Pseudo-code of PANOIS algorithm based on BFF.

$\mathcal{G}_{\mathrm{s}}^{\star} = \left\{ \underset{i \in \mathcal{G}}{\mathrm{argmax}} \lvert\lvert \mathbf{H}_i \rvert\rvert_{\mathrm{F}}^2 \right\};$	*Select first user*
$C_{\mathrm{s}}^{\star} = \log_2 \det \left(\mathbf{I} + \mathbf{H}_{\mathrm{s}}^{\star} \mathbf{R}_{\mathrm{s}}^{\star} \mathbf{H}_{\mathrm{s}}^{\star,H} \right);$	*Estimate capacity*
While $\lvert \mathcal{G}_{\mathrm{s}}^{\star} \rvert \leq N_{\mathrm{T}}/N_{\mathrm{r}}$ and $\lvert \mathcal{G}_{\mathrm{s}}^{\star} \rvert \leq N_{\mathrm{u}}$, **do**:	
$\mathcal{G}_{\mathrm{ns}} = \mathcal{G} \setminus \mathcal{G}_{\mathrm{s}}^{\star};$	*Non-scheduled users set*
For $k = 1, \ldots, \lvert \mathcal{G}_{\mathrm{ns}} \rvert,$	
$\mathcal{G}_{\mathrm{s}} = \mathcal{G}_{\mathrm{ns}}\{k\} \cup \mathcal{G}_{\mathrm{s}}^{\star};$	*Test set with added user*
$C_{\mathrm{s},k} = \log_2 \det \left(\mathbf{I} + \mathbf{H}_{\mathrm{s}} \mathbf{R}_{\mathrm{s}} \mathbf{H}_{\mathrm{s}}^{H} \right);$	*Estimate new capacity*
end-for	
$k^{\star} = \underset{k}{\mathrm{argmax}}\, C_{\mathrm{s},k};$	*Select user providing highest group capacity*
If $C_{\mathrm{s},k^{\star}} > C_{\mathrm{s}}^{\star},$	*If rate improves*
$\mathcal{G}_{\mathrm{s}}^{\star} = \mathcal{G}_{\mathrm{ns}}\{k^{\star}\} \cup \mathcal{G}_{\mathrm{s}}^{\star};$	*Scheduled group update*
$C_{\mathrm{s}}^{\star} = C_{\mathrm{s},k^{\star}};$	*Capacity update*
else	*No rate improvement*
break-while	*Stop algorithm*
end-if	
end-while	

Table 4.3: Complexity of search methods

Search Method	Max. # of combinations to evaluate
Exhaustive	$2^L - 1$
FFF	$L - 1$
BFF	$(L^2 - L)/2$

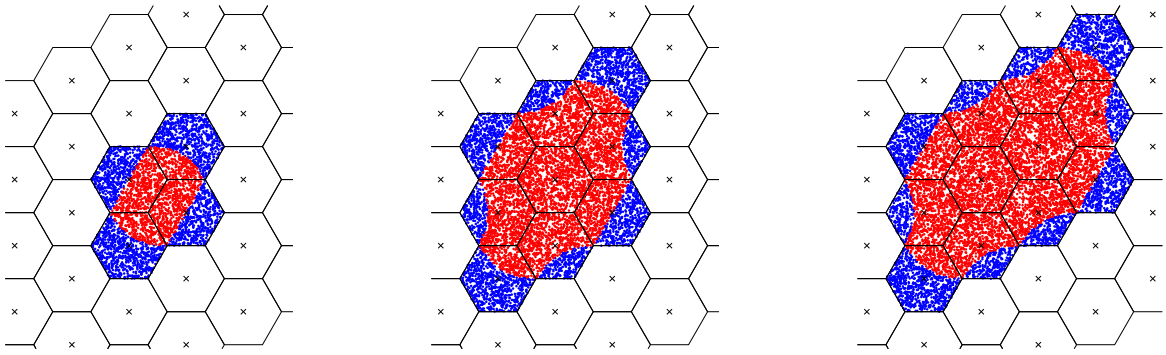

Figure 4.2: Interference dominance for different cluster sizes.

The IAPANOIS is intended to avoid such cases by adaptively switching between pure scheduling (when applying precoding is not worthwhile) and PANOIS approach. This adaptation can be done according to the OIR in eq. (4.4). The OIR estimate can be obtained by gathering long-term measurement reports from MSs. In each report the received power from the neighboring BSs must be reported by each MS to the cluster CPU which must be able to determine whether each power measurement refers to a BS within the cluster or not.

According to the measured OIR the IAPANOIS chooses the PANOIS approach when $\mathrm{OIR} < 1$, i. e. when the interference within the cluster is dominant compared to that coming from outside, otherwise it chooses a pure scheduling technique like NOIS, for instance. These procedure steps are ilustrated in Fig. 4.3.

4.5 Results

This section presents the results that compare our proposal algorithm, IAPANOIS, with ST-ZF, OIS-ZF and NOIS-ZF. These three last can be refered as *decoupled algorithms* – all consist of a BS scheduling followed by a ZF precoder without any linkage between scheduling and precoding procedures involved. The ZF precoder was also set as the internal precoder of IAPANOIS in orderto have a fair comparison, once the novelty is in how the proposed algorithm deal with these two already mentioned interference mitigatigation tools. Certainly a non-linear algorithm like

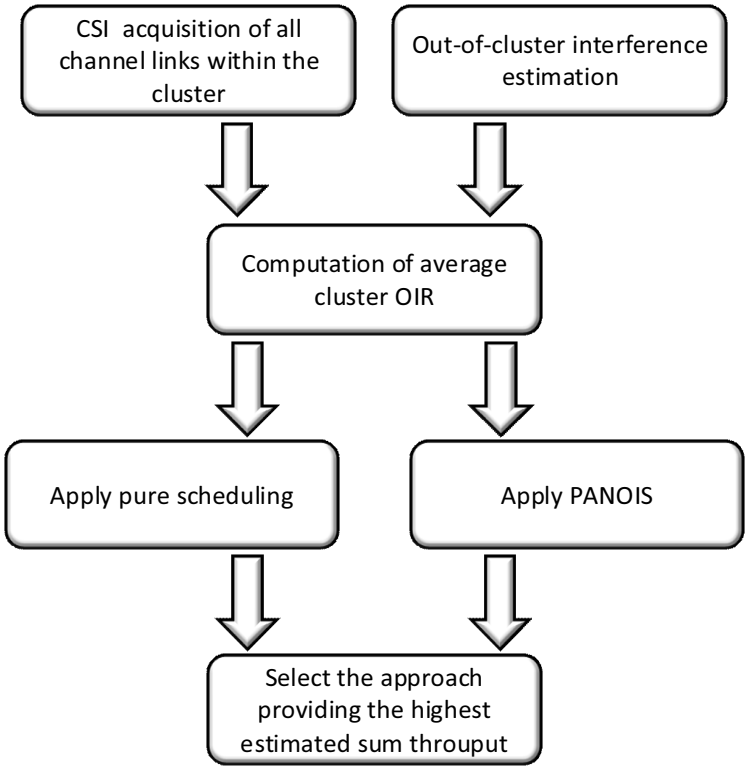

Figure 4.3: IAPANOIS block diagram

Table 4.4: Simulation Settings

Parameter	**Value**
Number of MSs per cell	1 or 5
Number of cells	36
Group size	1, 3, 4, 9, 12
Noise power	-115 dBm
Maximum BS Transmit Power	33 dBm
Number of snapshots	10000
Cell radius	1 km
Shadow fading std.	6 dB
Rayleigh fading	uncorrelated

ZF-THP would provide an even better result.

Some practical assumptions were made in the simulations, which include: perfect BS cooperation, perfect channel estimation at both transmitter and receiver sides, no reception delays, homogeneous cellular grid, per-base power constraints and single-antenna base and mobile stations. Further simulation parameters are shown in Table 4.4.

In order to induce significant OIR fluctuations, one computational way found was to make the cluster size to vary. The evaluated cluster sizes vary from 1 to 12 on a 36-cell grid, as illustrated in Fig. 4.4.

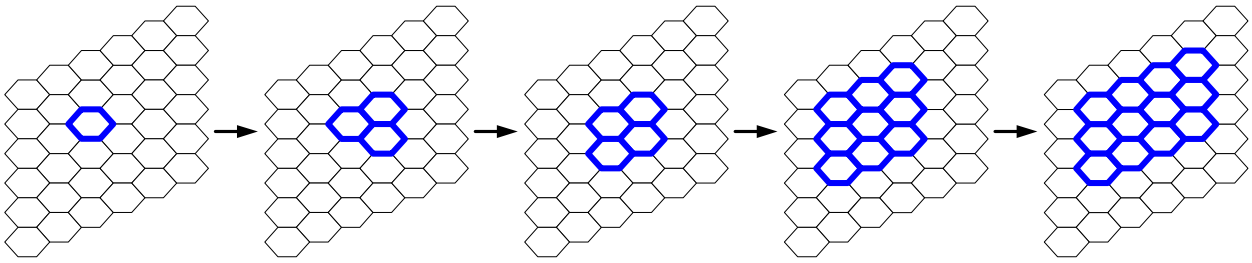

Figure 4.4: Illustration of cluster size analysis

Different experiments have been accomplished and divided in the three following subsections. The first shows how each strategy contributes for the average cell spectral efficiency, regardless the fact that there is no cooperation among clusters and hence any inter-cluster interference leakage will remain thus reducing significantly such an average cell spectral efficiency; the second subsection investigates the average sum spectral efficiency achieved per cluster – this normalization leads to different conclusions regarding the first situation; and finally the third subsection shows how the achieved MS spectral efficiency is distributed.

4.5.1 Average Cell Spectral Efficiency Evaluation

The Fig. 4.5 shows the impact of the number of cooperative cells per cluster on the achieved average spectral efficiency per cell. The results show that, except for IAPANOIS, when clusters are 3-cell larger or less the BS cooperation does not improve the average cell spectral efficiency. For clusters with more than 3 cooperative cells the algorithms NOIS-ZF and ST-ZF starts to improve compared to previous cluster configurations, but both strategies show that is only worthwhile doing BS cooperation for clusters with more than 12 cells. On the other hand the OIS-ZF showed to have taken less advantage of BS cooperation, as expected once it schedules just one BS per cluster no matter how large it is, causing a deep loss in the average cluster spectral efficiency and hence in the average cell spectral efficiency, as well.

Differently, from the other techinques being compared, our proposed algorithm actually took advantage of BS cooperation and not only outperformed all of them but kept stable the target measure, the average cell spectral efficiency, with the increase of cluster size.

4.5.2 Average Cluster Spectral Efficiency Evaluation

The Fig. 4.6 shows a similar analysis to the one in the previous subsection. The major difference is that the overall system sum soectral efficiency has been averaged according to the current cluster size being assessed, thus highlighting the behaviour of the avergae cluster sum spectral efficiency, which was early told to be our principal aim to improve such a measure.

These results show that BS cooperation was able to improve rates achieved by all strategies considered. Although, IAPANOIS was shown to had better taken advantage of such a cooperation and kept itself relatively far better the others if the output numbers along wth it lower computational complexity are both regarded.

4.5.3 Average MS Spectral Efficiency Distribution Evaluation

The Fig. 4.7 shows that not only in terms of average cluster spectral efficiency, our proposed algorithm, IAPANOIS, keeps a reasonable fairness concerning the rates achieved by all MSs. The fact that it appears behind the OIS-ZF in these results does not have much significance, once the OIS scheduler was always expected to provide the fairest outcomes due to its hard criterium of BS scheduling that reduces drastically the cluster-inner interference at the cost of the lowest rates compared to the other techniques.

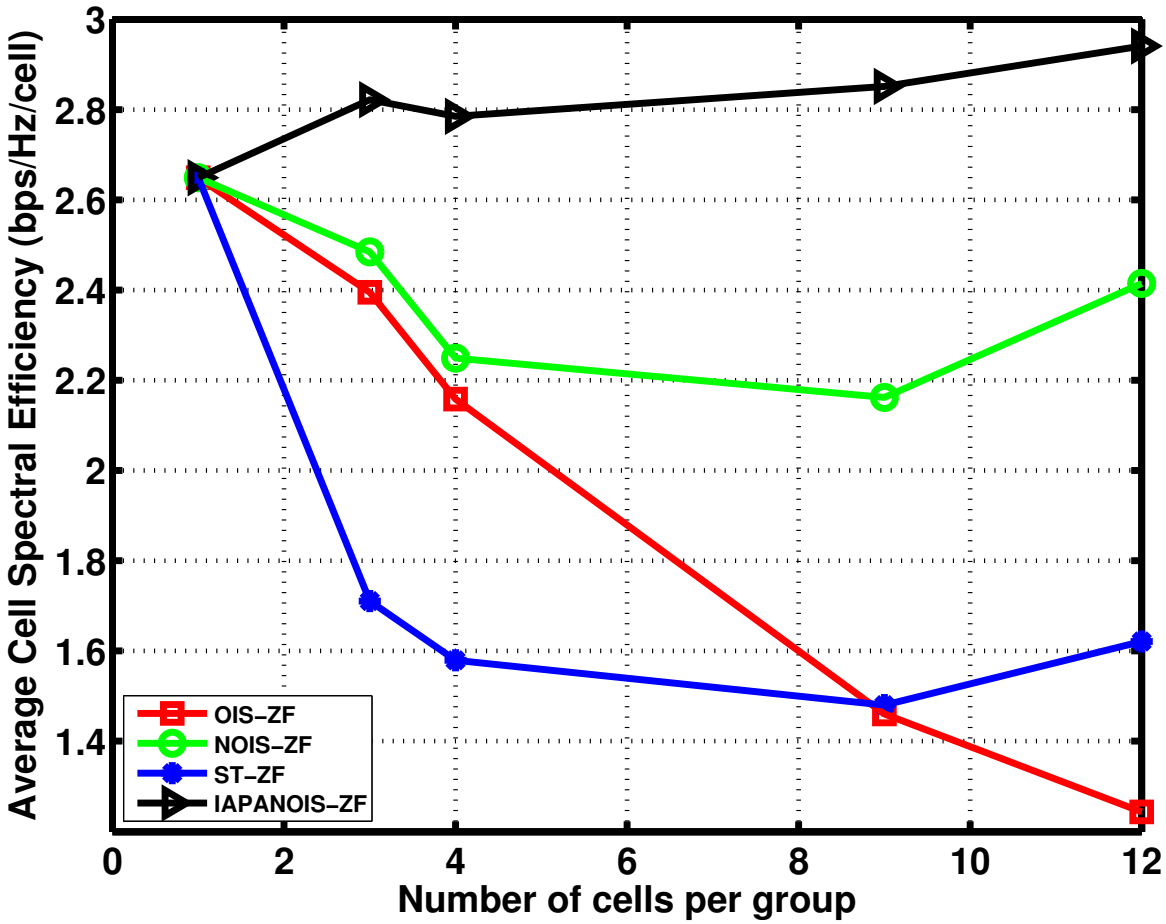

(a) One MS per cell

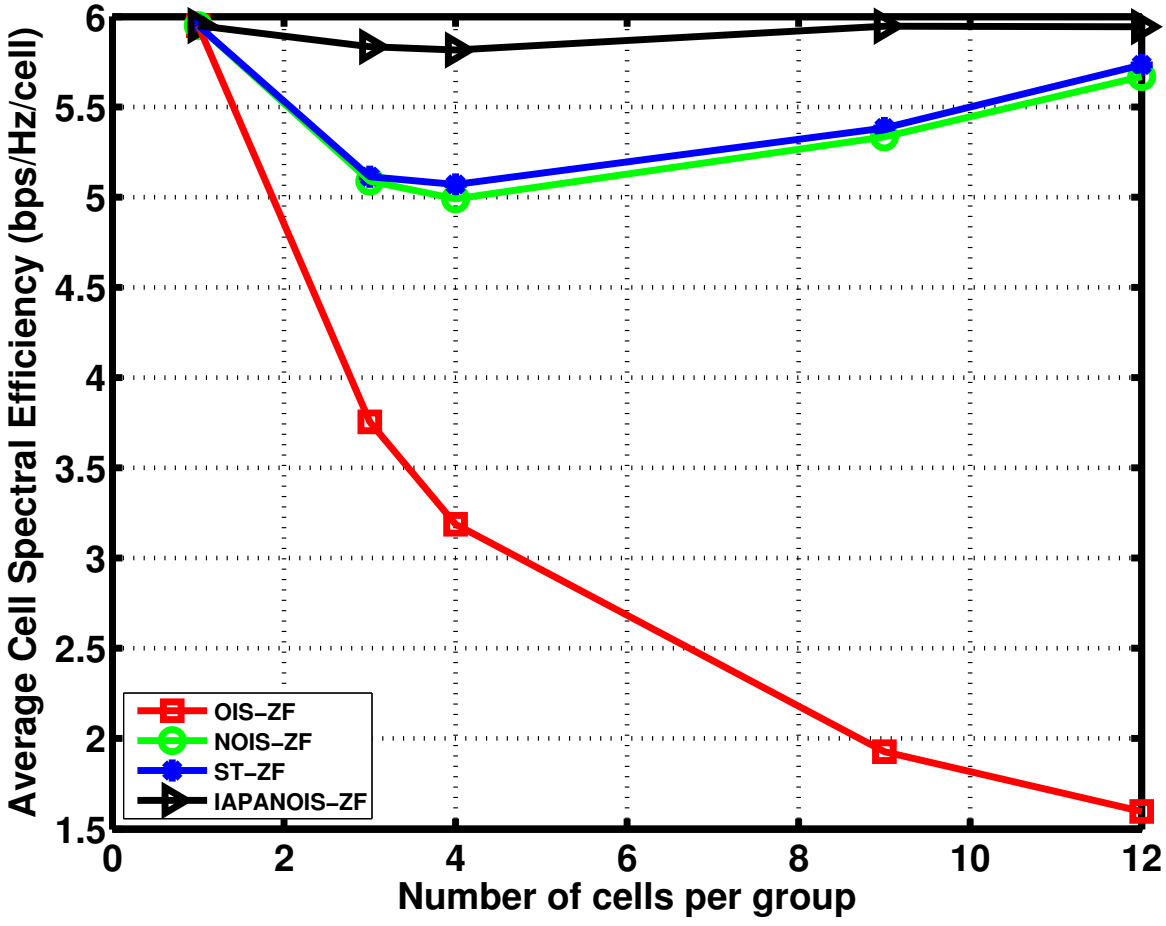

(b) Five MSs per cell

Figure 4.5: Impact of cluster size on average cell capacity

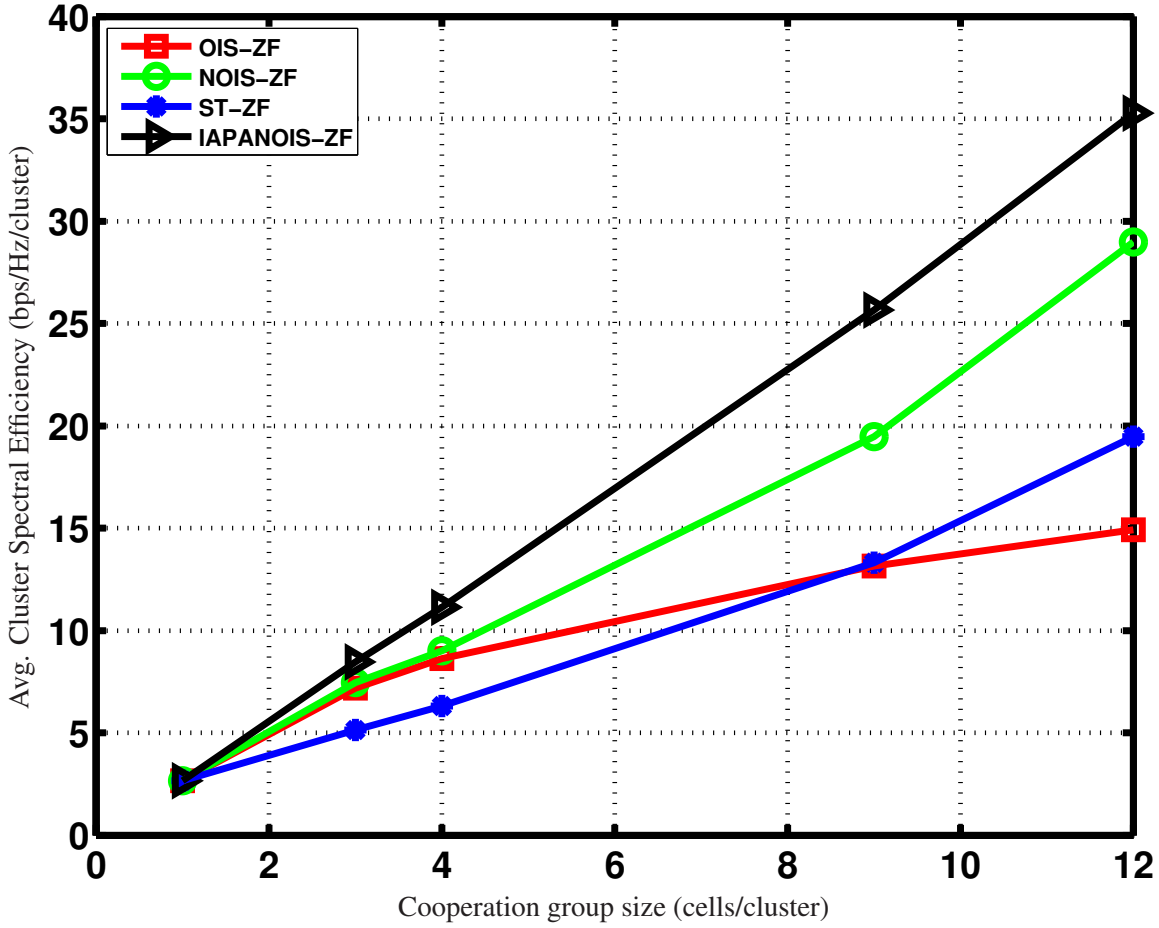

(a) One MS per cell

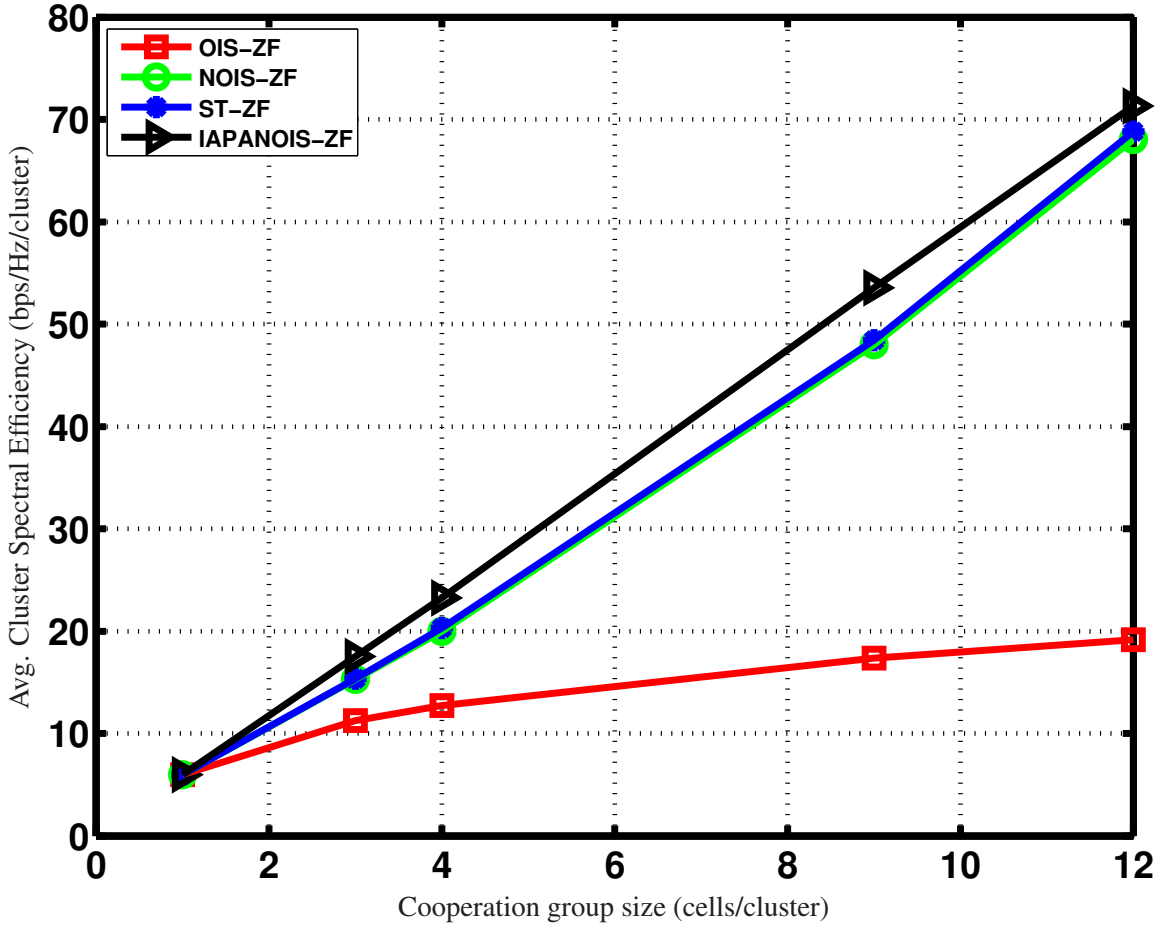

(b) Five MSs per cell

Figure 4.6: Impact of cluster size on average cluster capacity

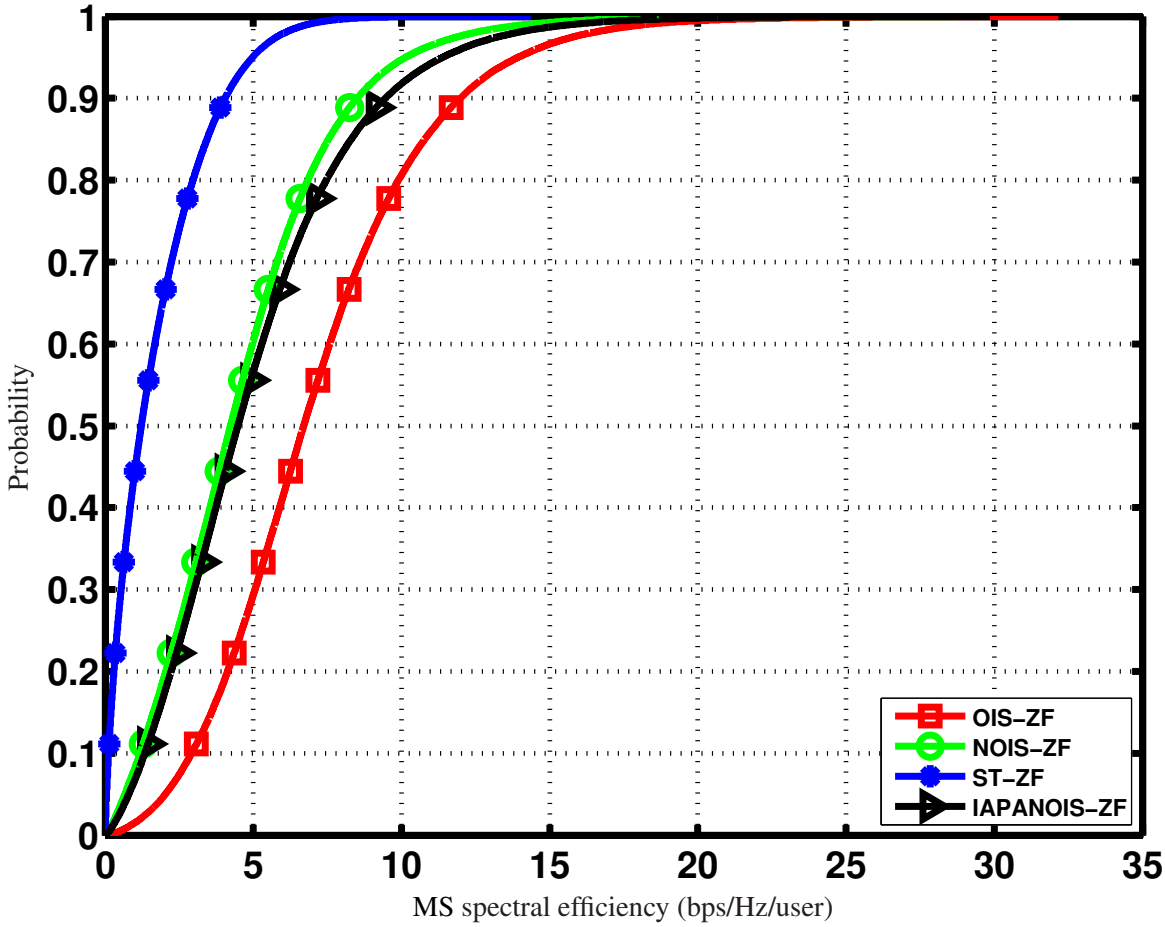

(a) CDF of MSs spectral efficiency assuming 1 MS per cell

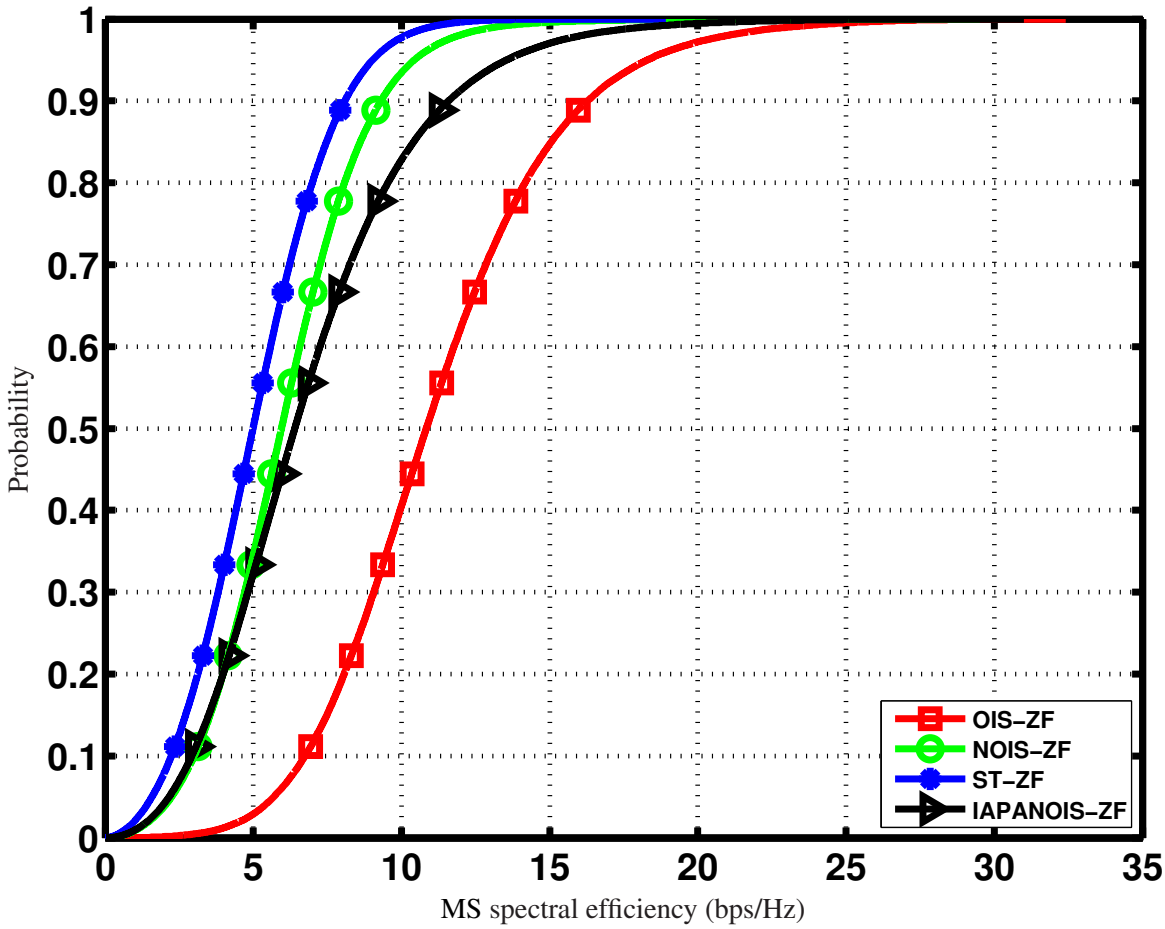

(b) CDF of MSs spectral efficiency assuming 5 MS per cell

Figure 4.7: CDF of the user capacity (1 user per cell and 3-cell cluster)

Chapter 5

Conclusions

In this Master's dissertation the problem of interference mitigation in a multi-cell multi-user has been faced and relevant contributions were reached. The main facts are pointed in the following.

In chapter 3 an investigation on the performance of different precoding techniques was assessed, assuming a scenario with one cluster formed by 3 cells whose BSs were allowed to cooperate so as to configure a distributed MIMO structure able to perform a precoded joint transmission. The results showed that under perfect CSI at transmitter and receiver sides, non-linear precoders save more transmit power and achieve higher rates than the linear ones, at the cost of being much more complex than these last. A channel estimation sensitivity evaluation was also regarded in order to see the behavior of each precoder with increasing channel perturbation. The results of this investigation were that under imperfect channel estimation at the transmitter side, only, all precoders converge to a same performance, except the BD to which was assumed a ZF filter in the receiver side with perfect channel estimation. If this assumption was not made about BD it would probably have the same result as the others, once it does a ZF but block-wise, separating MSs but not their own data streams (this last task was assumed to be accomplished in the receiver).

In the chapter 4, differently from chapter 3 not just only one cluster was considered but a 36-cell grid with several clusters, so as to tackle the out-of-cluster interference issue. In this chapter we proposed an algorithm, namely IAPANOIS, that was shown to outperform other strategies that made use of scheduling and precoding in a decoupled approach, i. e. without any level of coordination between the two procedures. IAPANOIS, instead, successively combines both scheduling and precoding approaches becoming a much powerful interference mitigation tool compared to the others. The results of this chapter shows that our proposal can outperform the other techniques in both average cluster and cell sum spectral effiencies at the same time keeping

resonable fair rates over the schedulued MSs.

List of acronyms

SCHEPTIC	SCHeduled Precoding Tool for Interference Cancellation
AWGN	Additive White Gaussian Noise
MAC	Multi-Access Control
AP	Access Point
BS	Base Station
MS	Mobile Station
SNR	Signal-to-Noise Ratio
SINR	Signal to Interference plus Noise Ratio
MIMO	Multiple Input Multiple Output
SISO	Single Input Single Output
CPU	Cluster Processing Unit
CSI	Channel State Information
CCI	Co-Channel Information
MSE	Mean Square Error
MF	Matched Filter
ZF	Zero-Forcing
MMSE	Minimum Mean Square Error
BD	Block Diagonalization
OLP	Optimal Linear Precoder

THP	Tomlinson-Harashima Precoder
ZF-THP	Zero-Forcing based Tomlinson-Harashima Precoder
QRSIC	QR decomposition based Successive Interference Cancellation
ST	Simultaneous Transmission
OIS	Orthogonal Inter-Cell Scheduler
NOIS	Non-Orthogonal Inter-Cell Scheduler
HINOIS	Hierarchical Non-Orthogonal Inter-Cell Scheduler
SIC	Successive Interference Cancelation
PANOIS	Precoding-Aware Non-Orthogonal Inter-Cell Scheduler
IAPANOIS	Interference-Adaptive Precoding-Aware Non-Orthogonal Inter-Cell Scheduler
OIR	Outer Interference to Inner Interference Ratio
FFF	First Fit First
BFF	Best Fit First
VAA	Virtual Antenna Array

Bibliography

[1] M. Rahman, H. Yanikomeroglu, M. Ahmed, and S. Mahmoud, "Opportunistic nonorthogonal packet scheduling in fixed broadband wireless access networks," *EURASIP Journal on Wireless Communications and Networking*, vol. 2006, pp. 1–11, 2006.

[2] C. Koutsimanis, "Inter-cell interference coordination techniques for multi-cell ofdma networks supporting narrow band and elastic services," Master's thesis, Royal Institute of Technology (KTH), 2007.

[3] R. B. Moreira and F. R. P. Cavalcanti, "An hierarchical approach for inter-cell scheduling in interference-limited cellular networks," in *Proc. IEEE SPAWC*, July 2008, pp. 376–380.

[4] H. Zhang and H. Dai, "Cochannel interference mitigation and cooperative processing in downlink multicell multiuser MIMO networks," *EURASIP Journal on Wireless Communications and Networking*, vol. 2, pp. 222–235, 2004.

[5] K. K. G. J. Foschini and R. A. Valenzuela, "Coordinating multiple antenna cellular networks to achieve enormous spectral efficiency," in *IEEE Proceedings on Communications*, vol. 153, no. 4, Aug. 2006.

[6] U. G. Team, "Third technical report - interference management and resource allocation for next generation wireless communication systems," Federal University of Ceará (UFC), Tech. Rep., May. 2008.

[7] M. Joham and J. A. Nossek, "Linear transmit processing in MIMO communications systems," *IEEE Transactions on Signal Processing*, vol. 53, no. 8, pp. 2700–2712, Aug. 2005.

[8] Q. H. Spencer, A. L. Swindlehurst, and M. Haardt, "Zero-forcing methods for downlink spatial multiplexing in multiuser MIMO channels," *IEEE Transactions on Signal Processing*, vol. 52, pp. 461–471, Feb. 2004.

[9] M. Tomlinson, "New Automatic Equalizer Employing Modulo Arithmetic," *Electronics Letters*, vol. 7, pp. 138–139, Mar. 1971.

[10] H. Harashima and H. Miyakawa, "Matched-Transmission Technique for Channels With Intersymbol Interference," *IEEE Transactions on Communications*, vol. 20, no. 4, pp. 774–780, Aug. 1972.

[11] R. F. H. Fischer, C. Windpassinger, A. Lampe, and J. B. Huber, "Space-time transmission using Tomlinson-Harashima precoding," *in Proc. ITG Conference on Source and Channel Coding (SCC)*, pp. 139–147, Jan. 2002.

[12] M. Joham, D. A. Schmidt, H. Brunner, and W. Utschick, "A symbol-wise order optimization for successive precoding," *in Proc. ITG/IEEE Workshop on Smart Antennas (WSA)*, Feb. 2007.

[13] B. M. Hockwald, C. B. Peel, and A. L. Swindlehurst, "A vector-perturbation technique for near-capacity multiantenna multiuser communication - part II: Perturbation," *IEEE Transactions on Communications*, vol. 53, no. 3, pp. 537–544, Mar. 2005.

[14] M. Joham, "Optimization of linear and nonlinear transmit signal processing," Ph.D. dissertation, Technische Universität München, 2004.

[15] C. B. Peel, "Studies in multiple-antenna wireless communications," Ph.D. dissertation, Brigham Young University, 2004.

[16] R. F. H. Fischer, C. Windpassinger, A. Lampe, and J. B. Huber, "Space-time transmission using Tomlinson-Harashima precoding," *in Proc. ITG Conference on Source and Channel Coding (SCC)*, pp. 139–147, Jan. 2002.

[17] H. Sato, "An outer bound to the capacity region of broadcast channels," *IEEE Transactions on Information Theory*, vol. 24, no. 3, pp. 374–377, May 1978.

[18] N. Jindal, S. A. Jafar, S. Vishwanath, and A. Goldsmith, "Sum power iterative water-filling for multi-antenna Gaussian broadcast channels," in *Proc. Conference Record of the 36th Asilomar Conference on Signals, Systems and Computers (Asilomar '02)*, vol. 2, Nov. 2002, pp. 1518–1522.

[19] F. Shad, T. D. Todd, V. Kezys, and J. Litva, "Dynamic slot allocation (DSA) in indoor SDMA/TDMA using a smart antenna basestation," *IEEE/ACM Transactions on Networking*, vol. 9, no. 1, pp. 69–81, Feb. 2001.

Livros Grátis

(http://www.livrosgratis.com.br)

Milhares de Livros para Download:

Baixar livros de Literatura
Baixar livros de Literatura de Cordel
Baixar livros de Literatura Infantil
Baixar livros de Matemática
Baixar livros de Medicina
Baixar livros de Medicina Veterinária
Baixar livros de Meio Ambiente
Baixar livros de Meteorologia
Baixar Monografias e TCC
Baixar livros Multidisciplinar
Baixar livros de Música
Baixar livros de Psicologia
Baixar livros de Química
Baixar livros de Saúde Coletiva
Baixar livros de Serviço Social
Baixar livros de Sociologia
Baixar livros de Teologia
Baixar livros de Trabalho
Baixar livros de Turismo